nature communications

Article

https://doi.org/10.1038/s41467-025-57360-1

Crucial roles of Grr1 in splicing and translation of *HAC1* mRNA upon unfolded stress response

Received: 5 August 2024

Accepted: 20 February 2025

Published online: 04 March 2025

Check for updates

Nichika Sato[1], Yu Nakano[2], Yasuko Matsuki[2], Shota Tomomatsu[1], Sihan Li[1], Yoshitaka Matsuo[1] & Toshifumi Inada[1,2]

In the process of the unfolded protein response (UPR), the Hac1p protein is induced through a complex regulation of the *HAC1* mRNA. This includes the mRNA localization on the endoplasmic reticulum (ER) membrane and stress-triggered splicing. In yeast, a specific ribosome ubiquitination process, the monoubiquitination of eS7A by the E3 ligase Not4, facilitates the translation of *HAC1*^{i}, a spliced form of the *HAC1* mRNA. Upon UPR, the mono-ubiquitination of eS7A increases due to the downregulation of Ubp3, a deubiquitinating enzyme of eS7A. However, the exact mechanisms behind these regulations have remained unknown. In this study, an E3 ligase, Grr1, an F-box protein component of the SCF ubiquitin ligase complex, which is responsible for Ubp3 degradation, has been identified. Grr1-mediated Ubp3 degradation is required to maintain the level of eS7A monoubiquitination that facilitates Hac1p translation depending on the ORF of *HAC1*^{i}. Grr1 also facilitates the splicing of *HAC1*^{u} mRNA independently of Ubp3 and eS7A ubiquitination. Finally, we propose distinct roles of Grr1 upon UPR, *HAC1*^{u} splicing, and *HAC1*^{i} mRNA translation. Grr1-mediated Ubp3 degradation is crucial for *HAC1*^{i} mRNA translation, highlighting the crucial role of ribosome ubiquitination in translational during UPR.

Ribosome ubiquitination is a crucial modification of translation quality control pathways targeting the nascent polypeptide (RQC: Ribosome-associated Quality Control) and mRNA (NGD: No-Go Decay), as well as nonfunctional rRNA decay (18S NRD)[1–5]. In RQC, collision sensors Hel2 in yeast and ZNF598 in mammals form a K63-linked polyubiquitin chain on uS10 of the stalling ribosome in collided disomes or disomes[6–9]. The K63-linked polyubiquitin chain on uS10 is subsequently recognized by the RQC-trigger (RQT) complex and plays a crucial role in the dissociation of collided ribosomes into subunits to initiate the RQC pathway[6–12]. In yeast, the RQT complex is composed of the RNA helicase-family protein Slh1, ubiquitin-binding protein Cue3, and Rqt4[8]. The ATPase activity of Slh1 is responsible for subunit dissociation of polyubiquitinated collided ribosomes[8,10]. The two subunits of the RQT complex, Cue3, and Rqt4 simultaneously recognize the K63-linked polyubiquitin chain formed on the stalling ribosome by Hel2[11]. Similarly, ZNF598, the human homolog of Hel2, ubiquitinates ribosomal proteins uS10 and eS10 to initiate RQC in mammals. The human RQT (hRQT) complex is composed of the RNA helicase-family protein ASCC3, the ubiquitin-binding protein ASCC2, and TRIP4[6,12], which specifically recognizes the K63-linked polyubiquitin chain on uS10 in collided ribosomes, indicating that the triggering step of RQC is conserved from yeast to humans[6].

The ubiquitination of the small subunit protein eS7A plays a crucial role in NGD[9]. Collided ribosomes are also subjected to the NGD pathway, which can be divided into two branches, depending on their coupling with RQC. NGD coupled with RQC is referred to as NGD^{RQC+}, depending on the Hel2-mediated K63-linked polyubiquitination of uS10 and RQT-mediated subunit dissociation of the stalling ribosomes[9].

[1]Division of RNA and gene regulation, Institute of Medical Science, The University of Tokyo, Minato-Ku, Tokyo 108-8639, Japan. [2]Graduate School of Pharmaceutical Sciences, Tohoku University, Sendai, Japan. e-mail: toshiinada@ims.u-tokyo.ac.jp

An endonuclease Cue2 is responsible for the cleavage at the vicinity of the collided ribosome[13,14]. In the absence of the subunit dissociation, the endonucleolytic mRNA cleavages upstream of the collision site are referred to as the NGD^{RQC-}. The cleavages in NGD^{RQC-} require K63-linked polyubiquitination of ribosomal protein eS7A via a two-step mechanism, the E3 ligase Not4 first monoubiquitinates eS7A which is then followed by Hel2-mediated polyubiquitination[14]. Polyubiquitination of eS7A is required for the recruitment of Cue2, which cleaves mRNA upstream of the collided ribosomes[14].

Despite an increased understanding of the role of ribosome ubiquitination in quality control pathways, the physiological relevance of ribosome ubiquitination remains largely unknown. The Ccr4-Not complex initiates mRNA decay through the deadenylation and activation of decapping[15,16]. The Ccr4-Not complex monitors the translating ribosome for codon optimality via a specific interaction of the Not5 subunit with the ribosomal E-site[17]. This interaction only occurs when the ribosome lacks an accommodated A-site tRNA, indicative of low codon optimality. Ccr4-Not also interacts with the ribosome through mono-ubiquitination of eS7A by Not4 E3 ligase[9,14,18–20]. Deletion of Not4 and mutation of the four lysine residues targeted by Not4 (eS7A-4KR) strongly stabilized non-optimal and semi-optimal reporters[17]. This suggests that eS7A-ubiquitination is part of the same pathway as Not5-mediated sensing of translation rate, but occurs upstream of E-site probing, and the precise role of eS7A ubiquitination in codon optimality-dependent mRNA decay by Ccr4-Not remains elusive.

In recent studies, ribosomal ubiquitination has been linked to cellular responses to stress. K63 polyubiquitination may modulate oxidative stress responses, and ubiquitination of specific lysine residues in ribosomal proteins contributes to stress responses[19,21–28]. When cellular stresses lead to the accumulation of misfolded proteins within the endoplasmic reticulum (ER), it triggers a network of intracellular signaling pathways known as the unfolded protein response (UPR)[29–31]. In the UPR signaling pathway, *HAC1* mRNA in budding yeast[32–34] or *XBP1* mRNA in metazoans[32–34] is targeted to the ER-resident protein kinase and endonuclease Ire1[32,35,36]. Subsequently, Ire1 cleaves an intervening sequence from *HAC1/XBP1* mRNA, and the spliced form of *HAC1/XBP1* mRNA encodes a transcription factor that stimulates the expression of numerous proteins, including ER-resident chaperones, to upregulate the protein-folding capacity of the cell. Induction of the UPR upregulates the ubiquitination of ribosomal proteins in mammals[37] and yeast[18]. In yeast, the ubiquitination of eS7A, uS10, and uS3 was upregulated and Not4-mediated monoubiquitination of eS7A is required for resistance to tunicamycin (Tm), whereas E3 ligase Hel2-mediated polyubiquitination of uS10 and uS3 is not required[18]. Ribosome profiling revealed that monoubiquitination of eS7A is crucial for translational regulation, including upregulation of the spliced form of *HAC1* ($HAC1^i$) mRNA[18]. Downregulation of the deubiquitinating enzyme complex Ubp3-Bre5 increased the levels of ubiquitinated eS7A during UPR[18]. These results suggest that monoubiquitination of ribosomal protein eS7A plays a crucial role in translational control during the ER stress response in yeast. However, it remains unknown how Ubp3 is downregulated and how eS7A ubiquitination facilitates $HAC1^i$ mRNA translation upon UPR.

In this study, we identified an E3 ligase, Grr1, an F-box protein component of the SCF ubiquitin ligase complex responsible for Ubp3 downregulation during the UPR. Grr1 is required for proteasomal degradation of Ubp3, thereby increasing levels of ubiquitinated eS7A. eS7A ubiquitination facilitates $HAC1^i$ translation during UPR. Collectively, we propose that upon UPR, Grr1-mediated proteasomal degradation of Ubp3 upregulates eS7A mono-ubiquitination, thereby promoting $HAC1^i$ translation. We also found that Grr1 facilitates the splicing of $HAC1^u$ mRNA independently of Ubp3 and eS7A ubiquitination, indicating the unknown function of SCF^{Grr1} complex in the mRNA splicing on the ER membrane.

Results

Grr1 is responsible for the proteasomal degradation of Ubp3 and facilitates $HAC1^u$ splicing upon UPR

Ribosome ubiquitination increases significantly upon induction of the UPR in mammals and yeast[18,37]. In yeast, Ubp3 is the enzyme responsible for deubiquitylation of the ubiquitinated eS7A and is downregulated, which is consistent with the increased level of monoubiquitinated eS7A in response to UPR[18]. To understand how ribosome ubiquitination is regulated upon UPR in yeast, we performed genetic screening of E3 ubiquitin ligases that are required for Tm-resistance growth and Ubp3 degradation. Among 76 deletion mutants of the E3 ligases, we identified *pep3*Δ and *grr1*Δ mutants that conferred Tm-sensitive growth (Fig. 1A and Supplementary Fig. 1A). The level of Hac1 protein (Hac1p), an essential transcription factor induced by ER stress, was downregulated in the *grr1*Δ mutant, 4 h after Tm treatment (Fig. 1B, lanes 1-8). In contrast, the level of Hac1p was not decreased in the *pep3*Δ mutant cells (Fig. 1B, lanes 9-12). In the *grr1*Δ and *pep3*Δ mutant cells, induction of *HAC1* mRNA by Tm treatment was intact (Fig. 1C). We quantified the splicing efficiency based on the levels of unspliced $HAC1^u$ and spliced $HAC1^i$ forms of *HAC1* mRNA (Supplementary Fig. 1B–E), and the splicing efficiency in the *grr1*Δ mutant cells 2 h after Tm treatment was 52% of that in WT cells (Supplementary Fig. 1E), indicating that the splicing efficiency of *HAC1* mRNA is moderately reduced. The level of $HAC1^i$ mRNA in *grr1*Δ mutant cells was 40% of that in *GRR1* wildtype cells (Supplementary Fig. 1D), suggesting that Grr1 also contributes to Hac1p expression upon UPR at the post-transcriptional levels.

Grr1 is the F-box protein component of an SCF ubiquitin-ligase complex[38,39]. Therefore, we hypothesized that the upregulated Ubp3 decreases the monoubiquitinated eS7A in the *grr1*Δ mutant cells, thereby reducing the Hac1p level. The level of Hac1p 2 h after Tm treatment was reduced in the eS7A ubiquitination-defective *eS7A-4KR* cells, confirming that monoubiquitination of ribosomal protein eS7A plays a crucial role in translational control during the ER stress response in yeast (Supplementary Fig. 1F). Neither uS3 nor uS10 ubiquitination, which is essential for 18S NRD and RQC, affected the Hac1p level upon UPR (Supplementary Fig. 1G, H), indicating that eS7A ubiquitination plays a crucial role in ER stress response. The downregulation of Ubp3 was diminished in *grr1*Δ mutant cells (Fig. 1D, lanes 9-12), indicating that Grr1 is required for Ubp3 downregulation upon UPR. To examine whether Ubp3 is subjected to Grr1-dependent proteasomal degradation, we measured Ubp3-3HA stability using cycloheximide (CHX) chase followed by western blotting (Fig. 1E). Ubp3-3HA was more unstable 2 h after Tm treatment (Fig. 1E, lanes 6-10; half-life, t1/2 ~ 80 min, Fig. 1G and Supplementary Fig. 2A) than in the absence of ER stress (Fig. 1E, lanes 1-5; half-life, t1/2 ~ 120 min, Fig. 1G and Supplementary Fig. 2A). We also noticed that Ubp3-3HA was not efficiently degraded 4 h after Tm treatment in wildtype and the *grr1*Δ mutant cells (half-life, $t_{1/2} > 120$ min, Supplementary Fig. 2C, D). Although Ubp3 is proposed to be involved in ribophagy[27], Ubp3-3HA was not stabilized in the *atg1*Δ mutant cells (Supplementary Fig. 3A, B) regardless of Tm treatment. However, Ubp3-3HA was stabilized after treatment with the proteasome inhibitor MG132 (Supplementary Fig. 3C, D, lanes 6-10) and in *grr1*Δ mutant cells regardless of Tm treatment (Fig. 1F, lanes 1-10; half-life, $t_{1/2} > 120$ min; Fig. 1G and Supplementary Fig. 2B). Moreover, RNA-seq and Ribo-seq demonstrated that levels of total and translated *UBP3* mRNAs were not reduced 4 h after Tm treatment (Supplementary Fig. 3E, F). These results demonstrated that Grr1 is responsible for the efficient degradation of Ubp3, which may contribute to efficient $HAC1^i$ translation probably via an increase in eS7A ubiquitination.

Grr1 interacts with Ubp3

Grr1 associates with core SCF (Cdc53p, Skp1p, and Hrt1p/Rbx1p) to form the SCF^{Grr1} complex[33,38–40]. The F-box domain was responsible for

https://doi.org/10.1038/s41467-025-57360-1

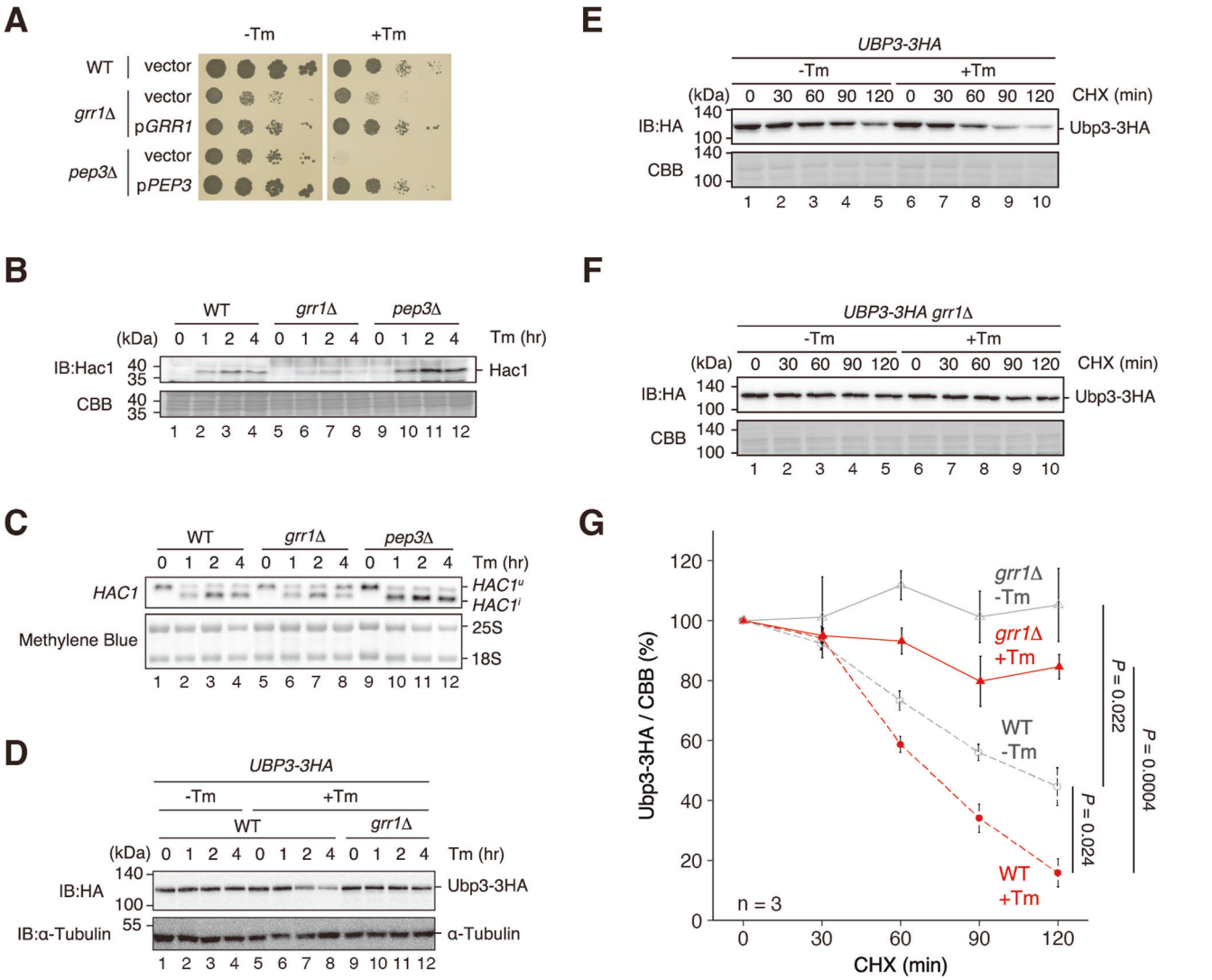

Fig. 1 | Grr1 is required for tunicamycin resistance, Hac1p expression and Ubp3 degradation in ER stress conditions. A *grr1*Δ and *pep3*Δ strains are sensitive to tunicamycin (Tm). Yeast cells lacking one of the E3 ligases and strains transformed with plasmids encoding each wild type were grown in SDC-Leu medium. 10-fold serial dilutions of OD_{600} = 0.3 cells were prepared in the 1.5 mL tubes and spotted onto Tm-added SDC-Leu and control plates. Plates were incubated at 30 °C for 2–3 days. **B** Hac1p expression is decreased in *grr1*Δ strains. Yeast cells were grown at 30 °C until OD_{600} = 0.2, then treated with 1 μg/mL of Tm for ~4 h and harvested. The samples were analyzed using western blotting with anti-Hac1 antibody. CBB staining was used as a loading control. **C** The splicing of *HAC1* mRNA occurs in *grr1*Δ and *pep3*Δ cells. Yeast cells were grown and harvested as in (**B**). The samples were analyzed by northern blotting with DIG-labeled *HAC1* probe. Methylene Blue staining was used as a loading control. **D** Ubp3 downregulation is suppressed in the *grr1*Δ cells. The indicated yeast cells expressing *UBP3-3HA* were grown and harvested as in (**B**). The samples were analyzed using western blotting with anti-HA and anti-α-Tubulin antibodies. **E**, **F** Grr1-dependent rapid decay of Ubp3 under ER stress conditions. The indicated yeast cells expressing *UBP3-3HA* were grown at 30 °C until OD_{600} = 0.2, then treated with 1 μg/mL of Tm for 1 h. Yeast cells were then treated with 0.25 mg/mL of cycloheximide (CHX) and harvested at the indicated times. The samples were analyzed with western blotting using anti-HA antibodies. CBB staining was used as a loading control. Dilutions are 100%, 75%, 50%, 25%, 12.5%, 6.25%. **G** The half-life of Ubp3-3HA in the wild-type and the *grr1*Δ mutant cells. The Ubp3-3HA/CBB levels shown in (**E**, **F**), Supplementary Fig. 2A, B were quantified and normalized relative to that at 0 min samples. Data represent $n = 3$ biologically independent experiments (mean ± SE), and P values were calculated by Two-sided Welch's t-test. All experiments were repeated at least twice with biologically independent samples and showed similar results. Source data are provided as a Source Data file.

binding to SCF, and the LRR domain interacted with the substrate for ubiquitination[38,39] (Fig. 2A). The levels of Ubp3-3HA upon UPR were determined in the *grr1*Δ cells expressing Grr1 mutants with the deletion of the indicated domains (Fig. 2B, C). The downregulation of Ubp3-3HA was diminished in the *grr1*Δ mutants expressing Grr1 mutant proteins that lack the 311-361 residues F-box (Fbox) and the 413-740 residues LRR (LRR) domains (Fig. 2B, lanes 9-12). The quantification of Ubp3-3HA levels revealed that the reduction of Ubp3-3HA by 4 h Tm treatment was diminished in *grr1*Δ mutant cells and complemented by plasmids expressing wildtype Grr1 or Grr1-ΔN but not by Grr1-ΔFbox or Grr1-ΔLRR mutant proteins (Fig. 2B, C and Supplementary Fig. 4A). We also determined the stability of Ubp3-3HA in the *grr1* mutant cells (Fig. 2D and Supplementary Fig. 4B). Ubp3-3HA destabilization by Tm treatment diminished in the *grr1*Δ mutant cells and complemented by plasmids expressing wildtype Grr1 or Grr1-ΔN but not by Grr1-ΔFbox or Grr1-ΔLRR mutant proteins (Fig. 2D and Supplementary Fig. 4B). Consistently, the *grr1*Δ mutants expressing Grr1-ΔFbox or Grr1-ΔLRR mutant conferred sensitivity to Tm (Fig. 2E) and the reduced Hac1p expression upon UPR (Fig. 2F). These indicated that the F-box and LRR domains of Grr1 are required for the downregulation of Ubp3-3HA upon UPR. The expression level of Grr1-ΔFbox or Grr1-ΔLRR mutant proteins was the same as the wild-type Grr1 (Fig. 2G). The expression level of Grr1-ΔN was significantly lower than that of wild-type Grr1 (Fig. 2G), but Grr1-ΔN complemented the *grr1*Δ

https://doi.org/10.1038/s41467-025-57360-1

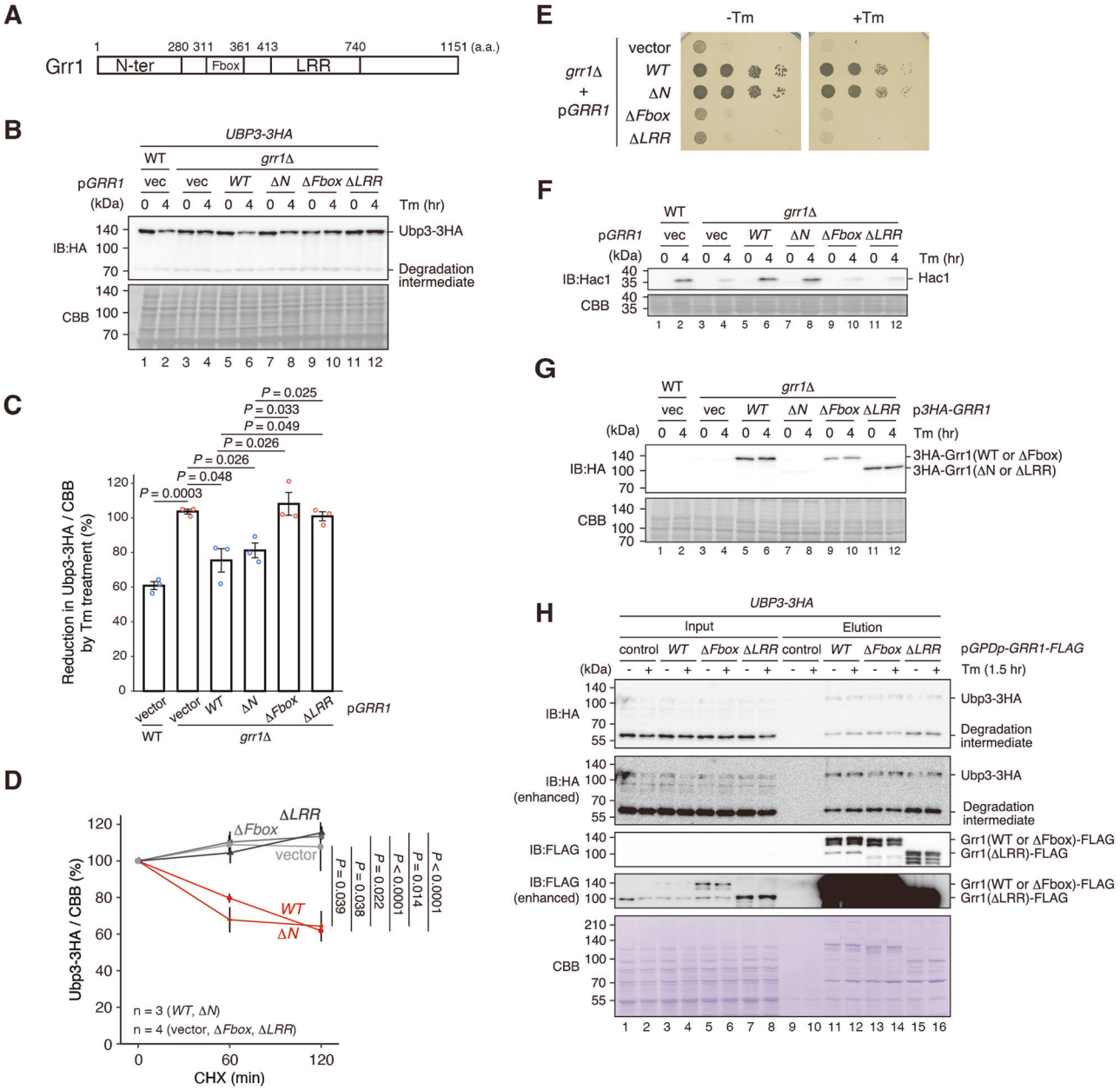

Fig. 2 | Fbox and LRR domains of Grr1 are crucial for its functions in ER stress conditions. A Schematic drawing of Grr1 domains. **B** Ubp3 downregulation is suppressed in the *grr1*Δ cells expressing *GRR1(ΔFbox)* and *GRR1(ΔLRR)* mutant. The *grr1*Δ mutant cells expressing the indicated *GRR1* mutants were grown and harvested as in Fig. 1B. The samples were analyzed using western blotting using anti-HA antibody. **C** The Ubp3-3HA/CBB levels shown in Supplementary Fig. 4A were quantified and normalized relative to that at 0 min samples. Data represent $n = 3$ biologically independent experiments (mean ± SE), and P values were calculated by Two-sided Welch's t-test. **D** The half-lives of Ubp3-3HA in the indicated Grr1 mutant cells. The Ubp3-3HA/CBB levels shown in Supplementary Fig. 4B were quantified and normalized relative to that at 0 min samples. Data represent at least three biologically independent experiments (mean ± SE), and P values were calculated by Two-sided Welch's t-test. **E** *GRR1(ΔFbox)* and *GRR1(ΔLRR)* mutant cells are sensitive to tunicamycin (Tm). The *grr1*Δ cells expressing the indicated *GRR1* mutants were grown in SDC-Ura medium. 10-fold serial dilutions of $OD_{600} = 0.3$ cells and spotted onto Tm-added SDC-Ura and control plates, then incubated at 30 °C for 2–3 days. **F** Hac1p is decreased in *GRR1(ΔFbox)* and *GRR1(ΔLRR)* mutant cells. Yeast cells were grown and harvested as in Fig. 1B. The samples were analyzed using western blotting using anti-Hac1 antibody. **G** Expression levels of Grr1p mutants. The *grr1*Δ cells expressing *3HA-GRR1* mutants were grown and harvested as in Fig. 1B. The samples were analyzed as in (**B**). **H** Grr1 was coimmunoprecipitated with Ubp3 independently of ER stress, F-box, and LRR domains. The yeast cells expressing Ubp3-3HA and the indicated Grr1-FLAG mutants were grown as in Fig. 1B, treated with 1 μg/mL of Tm for 1.5 h, and then harvested. Grr1-FLAG proteins were affinity-purified using anti-FLAG beads and FLAG peptides. The elution samples were analyzed by western blotting using anti-HA, anti-FLAG antibodies. All experiments were repeated at least twice with biologically independent samples and showed similar results. Source data are provided as a Source Data file. CBB staining was used as a loading control on western blot analysis in (**B**, **F**, **G**).

mutant phenotype in Tm sensitivity (Fig. 2E) and the reduced Hac1p level upon UPR (Fig. 2F), indicating that the N-terminal region is dispensable for Grr1 function. To confirm the interaction of Ubp3-3HA with Grr1, we purified the wild-type and mutant Grr1-FLAG proteins that lack F-box (ΔFbox) or LRR (ΔLRR) domains and examined the co-immunoprecipitation of the Ubp3-3HA (Fig. 2H). Ubp3-3HA co-immunoprecipitated with all Grr1 proteins (WT, ΔFbox, ΔLRR)(Fig. 2H, lanes 11-16), indicating that Grr1 interacts with Ubp3-3HA independent of the F-box and LRR domains. Taken together, we conclude that Grr1 destabilizes Ubp3 dependent on the F-box and LRR domains.

https://doi.org/10.1038/s41467-025-57360-1

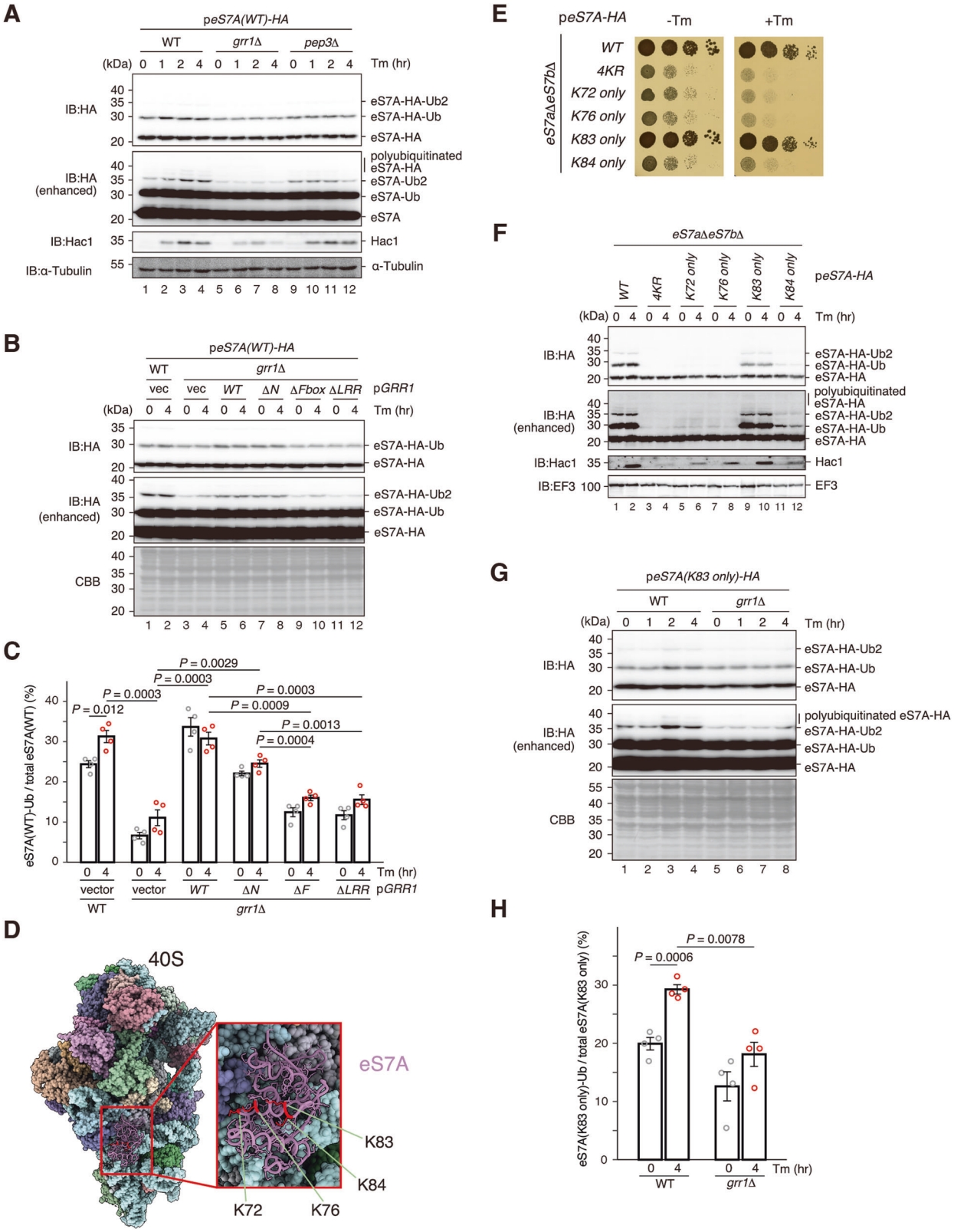

Grr1 facilitates eS7A ubiquitination

Not4-mediated monoubiquitination of eS7A is required to produce Hac1p during the UPR[18]; therefore, we assessed whether the upregulation of eS7A ubiquitination is dependent on Grr1. We found that the upregulation of eS7A ubiquitination diminished in *grr1*Δ mutant cells after the addition of Tm (Fig. 3A), indicating that Grr1 is required for the upregulation of eS7A ubiquitination upon UPR. In addition, the upregulation of eS7A ubiquitination partially attenuated in *pep3*Δ mutant cells after the addition of Tm (Fig. 3A). We also confirmed that defects in Ubp3 downregulation in the *grr1*Δ mutants expressing Grr1-ΔFbox or Grr1-ΔLRR proteins results in the reduction of eS7A monoubiquitination. The levels of mono- and diubiquitinated eS7A were reduced in *grr1*Δ cells (Fig. 3B, lanes 3-4) and *grr1*Δ cells expressing Grr1-ΔFbox or Grr1-ΔLRR mutants (Fig. 3B, lanes 9-12). The levels of

Fig. 3 | K83 of eS7A is a major ubiquitination site, and Grr1 is involved in this ubiquitination. A eS7A ubiquitination is decreased in the *grr1*Δ cells. The indicated yeast cells expressing *eS7A-HA* were grown and harvested as in Fig. 1B. The samples were analyzed using western blotting using anti-HA, anti-Hac1 and anti-α-Tubulin antibodies. **B** eS7A ubiquitination is decreased in *GRR1(ΔFbox)* and *GRR1(ΔLRR)* mutants. The *grr1*Δ cells expressing the *GRR1* mutants and *eS7A-HA* were grown and harvested. The samples were analyzed as in (**A**). **C** The eS7A-HA levels shown in Supplementary Fig. 5A were quantified and normalized relative to that at 0 min samples. eS7A-Ub levels were normalized to total eS7A levels (eS7A-Ub and free eS7A). Data represent $n = 4$ biologically independent experiments (mean ± SE), and P values were calculated by Two-sided Welch's t-test. **D** The schematic view of eS7A ubiquitination sites. This image was prepared by UCSF ChimeraX software using PDB file 8CBJ[20]. **E** K83 of eS7A is essential for tunicamycin resistance. *eS7a*Δ*eS7b*Δ cells expressing the indicated *eS7A-HA* mutants were grown in YPD medium. 10-fold serial dilutions of $OD_{600} = 0.3$ cells were prepared in the 1.5 mL tubes and spotted onto Tm added YPD and control plates. Plates were incubated at 30 °C for 2–3 days. **F** K83 of eS7A is a major ubiquitination site and essential for Hac1p expression. *eS7a*Δ*eS7b*Δ cells expressing *eS7A-HA* mutants were grown and harvested as in (**A**). The samples were analyzed using western blotting with anti-HA, anti-Hac1 and anti-EF3 antibodies. **G** eS7A ubiquitination at K83 is decreased in *grr1*Δ strains. Yeast cells harboring plasmids encoding *eS7A(K83 only)-HA* were grown and harvested as in (**A**). The samples were analyzed using western blotting with anti-HA antibody. CBB staining was used as a loading control. **H** The eS7A-HA levels shown in Supplementary Fig. 5B were quantified and normalized relative to that at 0 min samples. eS7A-Ub levels were normalized to total eS7A levels (eS7A-Ub and free eS7A). Data represent $n = 4$ biologically independent experiments (mean ± SE), and P values were calculated by Two-sided Welch's t-test. All experiments were repeated at least twice with biologically independent samples and showed similar results. Source data are provided as a Source Data file.

mono and di-ubiquitinated eS7A did not significantly change in *grr1*Δ cells expressing wild-type Grr1 and Grr1-ΔN mutant protein (Fig. 3B, lanes 5-8), in which Ubp3-3HA downregulation was partly restored (Fig. 2B). The quantification of the non-, mono-ubiquitinated eS7A proteins revealed that the ratio of monoubiquitinated eS7A was reduced in the *grr1*Δ mutant cells (Fig. 3C), and the reduction in the *grr1*Δ mutant cells was complemented by plasmids expressing wild-type Grr1 or Grr1-ΔN but not by Grr1-ΔFbox or Grr1-ΔLRR mutant proteins (Fig. 3C, Supplementary Fig. 5A, C). These are consistent with the stability of Ubp3-3HA in the *grr1* mutant cells (Fig. 2D and Supplementary Fig. 4B). Not4 monoubiquitinates eS7A at the four lysine residues (Fig. 3D)[41], with K83 ubiquitination primarily responsible for mRNA quality control[9]. We examined cell growth in the presence of Tm, eS7A ubiquitination, and Hac1p production upon UPR in four eS7A mutants containing a single lysine residue, susceptible to Not4-mediated monoubiquitination, *eS7A-K72only*, *eS7A-K76only*, *eS7A-K83only* and *eS7A-K84only*. K83 but no other lysine residues were responsible for resistance to Tm (Fig. 3E) and Hac1p expression upon UPR (Fig. 3F, middle panels). Consistently, K83 was found to be the major ubiquitination site of eS7A (Fig. 3F, top panels), confirming that K83 ubiquitination is primarily responsible for eS7A ubiquitination thereby Hac1p production upon UPR. We quantified the non-, mono-ubiquitinated eS7A proteins and demonstrated that the ratio of monoubiquitinated eS7A was reduced in the eS7A-K83only *grr1*Δ mutant cells (Fig. 3G, H, Supplementary Fig. 5B, D), indicating a crucial role of Grr1 in maintaining the level of eS7A ubiquitination at K83 upon UPR.

Grr1 is required for HAC1^i translation during the UPR in yeast

These results suggest that Grr1 plays a role in *HAC1* translation by downregulating Ubp3 during the UPR in yeast. To test whether Grr1 is involved in translational control of the UPR, we performed RNA-seq and ribosome profiling. To investigate the regulation of translation in response to ER stress, we estimated translation efficiency (TE) by assessing both mRNA abundance and ribosome occupancy. eS7A ubiquitination-dependent translational regulation was monitored at 4 h. Translational responses were observed in *grr1*Δ mutant cells, with statistically significant changes in the translation of *HAC1* mRNA (Fig. 4A, B; $Q < 0.05$). To examine the Grr1-mediated ubiquitination dependency of the involved mRNAs, TE fold-change by Tm treatment revealed 191 and 154 mRNAs categorized as up- and downregulated, respectively (Fig. 4B, C). These subsets were identified using the formula "log2 TE fold change (+ Tm) - log2 TE fold change (-Tm)", with mRNAs scored as > 2 and < −2 defined being up- and down-regulated, respectively.

We identified *HAC1* as the most significantly translationally upregulated gene during the UPR as previously reported[42,43] (Fig. 4A–D). In comparing TE in cells 4 h after the addition of Tm based on reads of *HAC1*, we found that the TE of *HAC1* mRNAs was approximately 1.96-fold lower in *grr1*Δ than in wild-type (WT) cells (Fig. 4C). The regulation of some of the *HAC1* target mRNAs[44–46] by Tm treatment was also affected in the *grr1*Δ mutant cells (Supplementary Fig. 6A). Ribo-seq demonstrated that the footprint on *HAC1^u* mRNA (Supplementary Fig. 6B, -Tm) was significantly lower than *HAC1^i* mRNA (Supplementary Fig. 6B, +Tm), indicating that translation of *HAC1^u* mRNA is inefficient. Given that the footprint on *HAC1^u* mRNA was low, the splicing efficiency of *HAC1^u* mRNA should affect TE. In the *grr1*Δ mutant cells, the splicing efficiency 4 h Tm treatment was 1.93-fold lower than WT (Supplementary Fig. 1E, 82.3% in WT, and 42.5% in *grr1*Δ), which could account for the 1.96-fold lower TE of *HAC1* mRNAs in *grr1*Δ than in wild-type (WT) cells. The footprints at the initiation codon were not changed in the *grr1*Δ mutant cells (Supplementary Fig. 6B), and the peaks in the 5′UTR were low and not changed in the mutant cells (Supplementary Fig. 6B), suggesting that translation initiation may not be affected. Mapping of the footprints throughout *HAC1^i* mRNA in WT and *grr1*Δ mutant cells *HAC1^i* mRNA contains potential translation pause sites (Fig. 4D), suggesting that Grr1 may be involved in translation elongation of *HAC1^i* mRNA.

Translation of HAC1^i mRNA requires eS7A ubiquitination regardless of ER stress

UPR induces the transcription and splicing of *HAC1^u* mRNA ensuring Hac1p expression upon UPR. We constructed a 5H3 clone containing the *HAC1* ORF, 5′ and 3′ untranslated regions (5′ and 3′ UTRs) but lacking an intron (Fig. 5A) and examined Hac1p levels in *hac1*Δ mutant cells harboring *5H3* clones under the control of various promoters (Fig. 5B). Hac1p is induced upon Tm treatment in *hac1*Δ mutant cells harboring *5H3* under the control of the *HAC1* promoter, as reported (Fig. 5B, lanes 5-6). Hac1p was expressed from *5H3* under the control of the *GPD*, *TEF1* and *ADH1* promoters, regardless of Tm treatment (Fig. 5B, lanes 7-12). Hac1p was induced upon UPR in *hac1*Δ mutant cells expressing *5H3* under the *CYC1* promoter (Fig. 5B, lanes 13-14), suggesting that *CYC1* transcription is induced upon UPR. We examined *HAC1* mRNA levels in *hac1*Δ mutant cells harboring *5H3* clones under the control of various promoters (Fig. 5C, D and Supplementary Fig. 7A–C). The transcriptional induction of *HAC1* and *CYC1* promoter by Tm treatment was confirmed. We also confirmed the expression levels of Hac1p in *hac1*Δ mutant cells harboring *5H3* clones under the control of various promoters were sufficient for Tm resistance (Fig. 5E).

We then examined whether eS7A ubiquitination is essential for the translation of *HAC1^i* mRNA without ER stress. Hac1p was expressed regardless of UPR in *eS7A-WThac1*Δ cells expressing *5H3* under the control of *HAC1* and *TEF1* promoters (Fig. 5F, lanes 5-6 and 9-10) but not in *eS7A-4KRhac1*Δ mutant cells that lack eS7A ubiquitination (Fig. 5F, lanes 7-8 and 11-12), indicating that eS7A ubiquitination is essential for translation of *HAC1^i* mRNA without ER stress. Upon UPR, the *HAC1* mRNAs expressed by *TEF1* promoter were increased 1.3-fold

https://doi.org/10.1038/s41467-025-57360-1

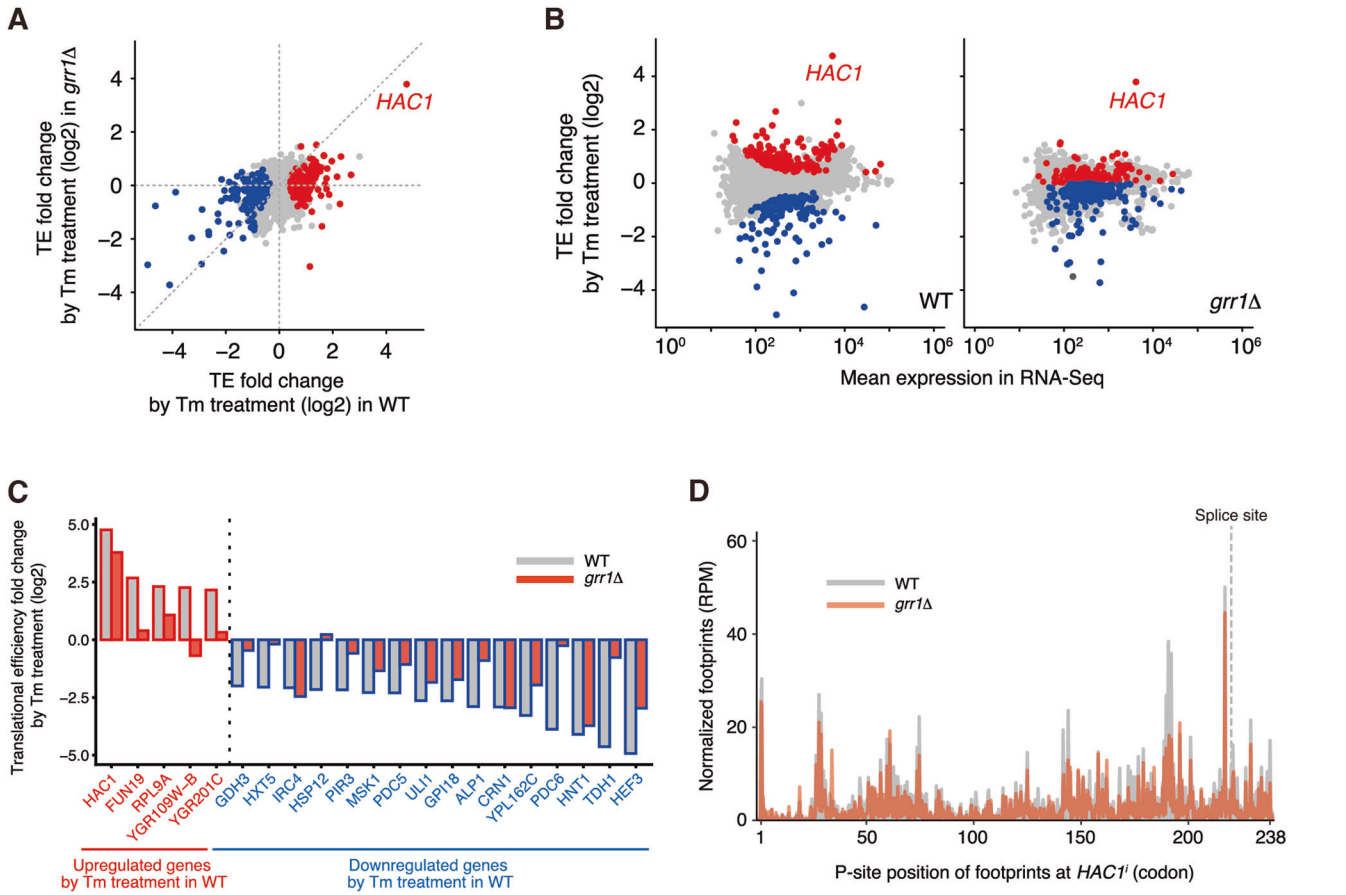

Fig. 4 | Grr1 is involved in efficient *HAC1*^{i} translation. A, **B** Fold change of translation efficiency (TE) in WT and *grr1*Δ cells. Red and blue dots represent genes with upregulated and downregulated TE in WT strains, respectively ($Q < 0.05$, calculated by Two-sided Likelihood ratio test). The ribosome profiling and RNA-seq results represent two independent biological replicates. **C** The genes with upregulated and downregulated TE in WT ($Q < 0.05$, calculated by Two-sided Likelihood ratio test). Genes with the log2 fold changes greater than 2 or less than −2 are shown. **D** Map of the P-site position of footprints at *HAC1*^{i} CDS in WT and the *grr1*Δ cells.

in *eS7A-WThac1*Δ but not increased in the *eS7A-4KRhac1*Δ cells (Fig. 5G, lanes 13-16, Fig. 5H and Supplementary Fig. 7C). In ER stress conditions, the levels of *HAC1* mRNAs in the *eS7A-WThac1*Δ cells were decreased 0.69-fold in *eS7A-4KRhac1*Δ cells (Fig. 5G, lanes 10 and 12, Fig. 5H). We then assessed the role of Grr1 in *HAC1*^{i} translation by using *5H3* constructs. Hac1p was expressed regardless of UPR in *grr1*Δ*hac1*Δ mutant cells expressing *5H3* under the control of *HAC1* and *TEF1* promoters (Fig. 5I, lanes 5-6 and 9-10). Importantly, Hac1p levels in *grr1*Δ*hac1*Δ cells (Fig. 5I, lanes 7-8 and 11-12) were lower than those in *hac1*Δ cells (Fig. 5I, lanes 5-6 and 9-10). We also determined *HAC1* mRNA levels in *hac1*Δ mutant cells harboring *5H3* clones under the control of *HAC1* and *TEF1* promoters (Fig. 5J). The *HAC1* mRNAs expressed by the *TEF1* promoter were moderately increased by Tm treatment in *hac1*Δ and not increased in *grr1*Δ*hac1*Δ cells (Fig. 5J, lanes 13-16, Fig. 5K and Supplementary Fig. 7D). In normal conditions, the levels of *HAC1* mRNAs in *hac1*Δ and *grr1*Δ*hac1*Δ cells were almost the same (Fig. 5J, lanes 13 and 15, Fig. 5K and Supplementary Fig. 7D), although the Hac1 protein was decreased in the *grr1*Δ*hac1*Δ cells than in *hac1*Δ cells (Fig. 5I, lanes 9 and 11), indicating that Grr1 facilitates translation of *HAC1*^{i} mRNA independent of ER stress.

ORF of HAC1^{i} mRNA is required for eS7A ubiquitination-mediated translation stimulation

To understand how eS7A ubiquitination facilitates *HAC1*^{i} mRNA translation under ER stress, we examined the putative *cis* elements required for the regulation. The *HAC1*^{i} mRNA 3′ UTR contains a cis-acting 3′-bipartite element (BE) at nucleotides C1134 to A1192 (adenine of the AUG codon is +1) that promotes co-localization of the translationally repressed *HAC1*^{i} mRNA under ER stress[47,48]. The protein kinases Kin1 and Kin2 contribute to *HAC1*^{u} mRNA processing by phosphorylation of Pal1 and Pal2 which bind to the 3′-BE of *HAC1* mRNA. *HAC1*^{u} mRNA is stored in the cytoplasm in the absence of ER stress, and its translation is tightly suppressed by a base-pairing interaction between the intron and the 5′ UTR. Excision of the intron by Ire1-dependent splicing in response to ER stress led to robust translation of *HAC1*^{i} mRNA, with the resulting Hac1p upregulating UPR target gene expression. We constructed *HAC1* with the deletion of 3′-BE or 5′-BP, a region responsible for base-pairing with 3′ UTR or both (Supplementary Fig. 8A, ΔBE, ΔBP, ΔBP + ΔBE). The Hac1p was induced 2 hrafter Tm addition in the *hac1*Δ mutant cells harboring the *5H3* clones under the control of the *HAC1* promoter (Supplementary Fig. 8B, lanes 5-12), indicating that these *cis* elements are not essential for the induction of Hac1p upon UPR. Consistently, *hac1*Δ mutant cells expressing *HAC1* conferred resistance to Tm similar to wild-type cells (Supplementary Fig. 8C).

To identify the cis-elements involved in eS7A monoubiquitination-dependent translation activation of *HAC1*^{i} mRNA, we constructed plasmids that contain the *HAC1*^{i} ORF with or without 5′ and 3′ UTRs of *HAC1* (Fig. 6A). The transcription from the *TEF1* promoter is terminated by the *CYC1* terminator in clones that contain the *HAC1*^{i} ORF without 3′ UTR of *HAC1*, and we named them *5HCt* and *HCt* due to *CYC1* terminator-mediated transcription termination. The *hac1*Δ mutant cells expressing

https://doi.org/10.1038/s41467-025-57360-1

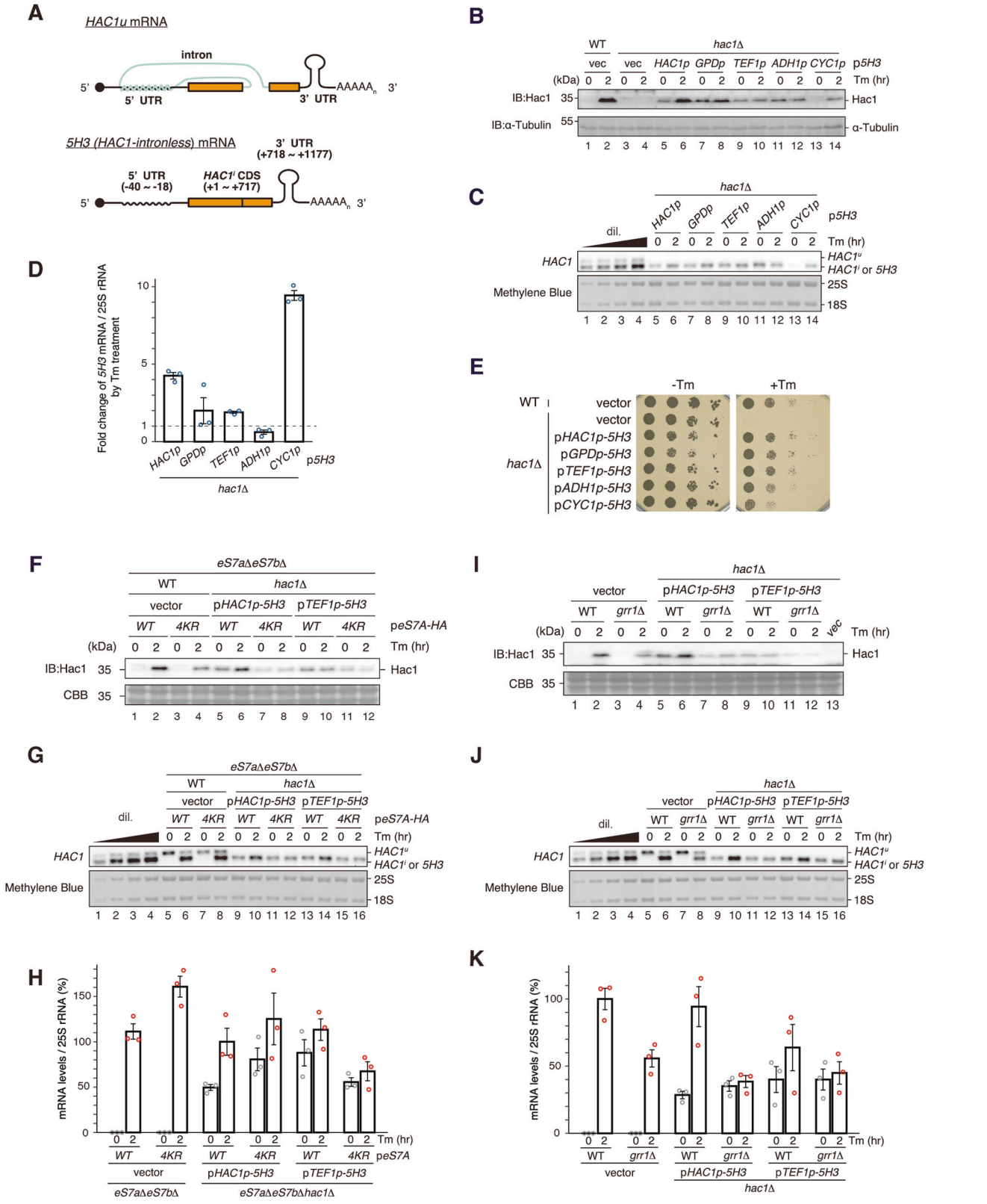

the *5H3*, *5HCt*, *H3*, and *HCt* mRNAs by the *TEF1* promoter (*TEF1p-5H3*, *5HCt*, *H3*, *HCt*) conferred resistance to Tm similar to wild-type cells (Fig. 6B), indicating that UTRs are dispensable for the expression of Hac1p by the *TEF1* promoter at a sufficient level for Tm resistance. The Hac1p was expressed in cells harboring *TEF1p-5H3*, *5HCt*, *H3*, and *HCt* clones (Fig. 6C, lanes 7-14). We extensively quantified and found that the levels of 3xFLAG-Hac1p were increased by 5′ and 3′ UTRs (Fig. 6C, lanes 7, 9, 11, 13; Fig. 6D). We examined the role of eS7A ubiquitination in Hac1p derived from these clones. The levels of 3xFLAG-Hac1p expressed in all *HAC1^i* clones were significantly diminished in *eS7A-4KR* cells (Fig. 6C, lanes 7-14; Fig. 6D and Supplementary Fig. 8D). We also quantified the *3xFLAG-HAC1* mRNAs expressed from *TEF1p-5H3*, *5HCt*, *H3*, and *HCt* clones in the *eS7A* and *eS7A-4KR* cells 2 h after Tm treatment (Fig. 6E, F). The *HAC1* mRNAs expressed from *TEF1p-5H3*, *5HCt*, *H3* were

Fig. 5 | eS7A ubiquitination is required for efficient Hac1p expression from *HAC1*^{i}. **A** Schematic drawing of *HAC1*^{u} mRNA and *5H3(HAC1-intronless)* mRNA. **B** Hac1p expression from *5H3* reporters with different promoters. Cells were grown and harvested and the samples were analyzed as in Fig. 1B. **C** Induction of *5H3* from various promoters by Tm treatment. Yeast cells were grown at 30 °C until OD_{600} = 0.2, then treated with 1 μg/mL of Tm for ~ 2 h and harvested. The samples were analyzed by northern blotting with DIG-labeled *HAC1* probe. Methylene Blue staining was used as a loading control. Dilutions are 100%, 75%, 50%, 25%. **D** Fold change of *5H3* mRNA/25S rRNA levels shown in Fig. 5C and Supplementary Fig. 7A, B were quantified and normalized relative to that at 0 min samples. **E** The correlation between Hac1p levels and tunicamycin resistance. 10-fold serial dilutions of OD_{600} = 0.3 cells grown in SDC-Ura medium were spotted onto SDC-Ura plates. Plates were incubated at 30 °C for 2–3 days. **F** eS7A ubiquitination is required for efficient Hac1p expression from *5H3* clones under control of *HAC1* or *TEF1* promoters. The indicated cells were harvested as in (**C**). The samples were analyzed as in Fig. 1B. **G** *HAC1*^{i} and *5H3* mRNA levels in *eS7A(WT)* and *eS7A(4KR)*. Yeast cells were harvested, and the total RNA samples were analyzed using northern blotting as in (**C**). **H** *5H3* mRNA/25S rRNA levels shown in (**G**) and Supplementary Fig. 7C were quantified and normalized relative to 2 h in *hac1*Δ encoding *HAC1p-5H3*. **I** Grr1 is required for efficient Hac1p expression from *5H3* under control of *HAC1* or *TEF1* promoters. Cells were harvested as in (**C**), and samples were analyzed as in (**F**). **J** *HAC1*^{i} and *5H3* mRNA levels in WT and *grr1*Δ. Yeast cells were harvested, and the samples were analyzed as in (**C**). **K** *5H3* mRNA/25S rRNA levels shown in (**J**) and Supplementary Fig. 7D were quantified and normalized relative to 2 h in WT. All experiments were repeated at least twice with biologically independent samples and showed similar results. Data represent $n = 3$ biologically independent experiments (mean ± SE). Source data are provided as a Source Data file.

moderately decreased in *eS7A-4KR* cells than in *eS7A* cells (Fig. 6E, lanes 5-10, Fig. 6F and Supplementary Fig. 8E). The *3xFLAG-HAC1* mRNAs expressed from *TEF1p-HCt* were moderately increased in the *eS7A-4KR* cells than in the *eS7A* cells (Fig. 6E, lanes 11-12, Fig. 6F). Given that 3xFLAG-Hac1p level was reduced in the *eS7A-4KR* cells (20% of WT, Fig. 6D), we suspected that translation efficiency of *HCt* was strongly reduced in *eS7A-4KR* cells. We constructed a *3xFLAG-GFP* clone that contains the *GFP* open reading frame (ORF) under the control of the *TEF1* promoter and the *CYC1* terminator, and we compared it with a similar *HCt* clone. The levels of 3xFLAG-GFP were not affected in the *eS7A-4KR* cells (Fig. 6G, H). In contrast, the 3xFLAG-Hac1 protein derived from the *HCt* clone was only 20% of the control level, although the mRNA level was increased in the *eS7A-4KR* cells (Fig. 6C–F). These findings support the model that eS7A ubiquitination facilitates the translation of *HAC1*^{i} mRNA, depending on potential cis-elements within the ORF. Inhibition of proteasome activity by MG132 treatment did not rescue the reduction of Hac1p in *eS7A-4KR* cells (Fig. 6I, J), suggesting that the downregulation of Hac1p in the *eS7A-4KR* mutant cells may not be due to the facilitation of proteasomal degradation of the Hac1p. Finally, we propose that eS7A ubiquitination facilitates the translation of *HAC1*^{i} mRNA depending on putative cis element(s) in the ORF.

Grr1 is required for eS7A ubiquitination-mediated translation stimulation

We then examined whether Grr1 facilitates the translation of *HAC1* mRNA dependent on *HAC1* ORF. To examine whether ORF of *HAC1* is responsible for the Grr1 mediated regulation, we determined 3xFLAG-Hac1p derived from the *HCt* clone and 3xFLAG-GFP derived from the *GFPCt* clone in *grr1*Δ cells (Fig. 7A and Supplementary Fig. 9A). In the *grr1*Δ mutant cells, Hac1 derived from *HCt* was at 43% of the control level, while 3xFLAG-GFP levels in the *grr1*Δ mutant cells were at 75% of those in the control cells (see Fig. 7A and Supplementary Fig. 9A), indicating that *HAC1* ORF is responsible for the Grr1-mediated regulation. We then examined the roles of eS7A ubiquitination and Grr1 in *HAC1* translation. we determined 3xFLAG-Hac1p derived from 5H3 clone in *eS7A-K83only*, *grr1*Δ*eS7A-K83only*, *eS7A-K83R*, *grr1*Δ*eS7A-K83R* cells (Fig. 7B, C and Supplementary Fig. 9B). The levels of 3xFLAG-Hac1p were decreased by the deletion of Grr1 in the *eS7A-K83only* cells, but not in *eS7A-K83R* cells, indicating that Grr1 facilitates *HAC1* translation in an eS7 ubiquitination-dependent manner. We also determined 3xFLAG-Hac1p derived from *HCt* clone in *ubp3*Δ, *ubp3*Δ*grr1*Δ cells (Fig. 7D, E and Supplementary Fig. 9C). The levels of 3xFLAG-Hac1p were not decreased by the deletion of Grr1 in the *ubp3*Δ cells, indicating that Grr1 facilitates *HAC1* translation in an *UBP3*-dependent manner. To examine whether the low Hac1 protein levels in the *grr1*Δ cells could result from protein degradation by proteosomes, we determined the stability of Hac1 protein in wild-type and *grr1*Δ cells 2 h after Tm treatment (Supplementary Fig. 9D, E). The half-life of 3xFLAG-Hac1p was not changed in *grr1*Δ cells, indicating that Hac1 degradation does not contribute to the Grr1-mediated downregulation upon UPR (Supplementary Fig. 9D, E). Finally, we performed in vitro translation using lysates prepared from *ski2*Δ and *ski2*Δ*grr1*Δ mutant cells (Fig. 7F–H). Translation of *2xPA-HAC1*^{i} mRNA was significantly reduced in the reaction using *grr1*Δ mutant lysates but translation of *2xPA-GFP* mRNA was not significantly reduced with in vitro translation using *ski2*Δ and *ski2*Δ*grr1*Δ mutant cell lysates (Fig. 7F–H). These strongly suggest Grr1 is required for translation of *HAC1*^{i} mRNA.

Discussion

Hac1p is expressed specifically in response to ER stress and its expression is ensured by the multi-step regulation of *HAC1* mRNA[30,49]. This includes localization to the ER membrane, tight repression of translation, and Ire1p-mediated splicing. During ER stress responses in yeast, ubiquitination of ribosomal protein eS7A is necessary for translational control of *HAC1*^{i} mRNA. The deubiquitinating enzyme complex Ubp3-Bre5 regulates eS7A ubiquitination[18], and UPR leads to an increase in the level of monoubiquitinated eS7A by the downregulation of Ubp3. In this study, we identified Grr1, a subunit of the SCF^{Grr1} complex, as the essential E3 ligase responsible for the downregulation of Ubp3 (Figs. 1, 2), which facilitates eS7A ubiquitination (Fig. 3) and the translation of *HAC1*^{i} (Figs. 4–7). Grr1 is co-immunoprecipitated with Ubp3 and is required for Ubp3 degradation, regardless of ER stress (Figs. 1, 2). The F-box and LRR domains of Grr1 are necessary for Ubp3 degradation but dispensable for the substrate binding (Fig. 2H). Grr1 is essential for the downregulation of Ubp3 during the UPR (Fig. 2B–D) and is critical for Hac1p expression (Fig. 2F) and Tm resistance (Fig. 2E). Notably, Grr1 mutants that are defective in Ubp3 downregulation (e.g., the Grr1-ΔFbox or Grr1-ΔLRR mutants) exhibited defects in Hac1p expression (Fig. 2F). Importantly, Grr1 is necessary for maintaining eS7A ubiquitination levels, regardless of Tm treatment (Fig. 3). Finally, we confirmed that in *ubp3*Δ and *eS7A-4KR* background, *GRR1* deletion could not reduce the Hac1p level (Fig. 7A–E and Supplementary Fig. 9A–C), indicating that Grr1 facilitates Hac1p expression in the eS7A ubiquitination and Ubp3-dependent manner. Based on our findings, we propose that Grr1-mediated Ubp3 degradation is crucial for maintaining eS7A ubiquitination during UPR. We observed the increase of eS7A mono-ubiquitination in wild-type cells expressing eS7A-HA (Fig. 3B, C) or eS7AK83 only-HA (Fig. 3G, H). Importantly, the levels of eS7A mono-ubiquitination were increased upon UPR in the *grr1*Δ mutant cells expressing wildtype Grr1 or Grr1-ΔN but not by Grr1-ΔF or Grr1-ΔLRR mutant proteins (Fig. 3B, C). Given that wildtype Grr1 or Grr1-ΔN could complement the *grr1*Δ mutant defects in Ubp3 downregulation and Hac1p expression and Tm sensitivity, we propose that Grr1 is crucial to maintain the level of eS7A mono-ubiquitination upon UPR that is required for Hac1p expression.

The SCF^{Grr1} complex plays a crucial role in nutrient uptake and cell proliferation by interacting with various targets[33,50]. The F-box Grr1 selects and discriminates substrates, in part, via its leucine-rich repeat (LRR) domain[33,38–40,50,51]. In the Grr1-mediated downregulation of Ubp3,

https://doi.org/10.1038/s41467-025-57360-1

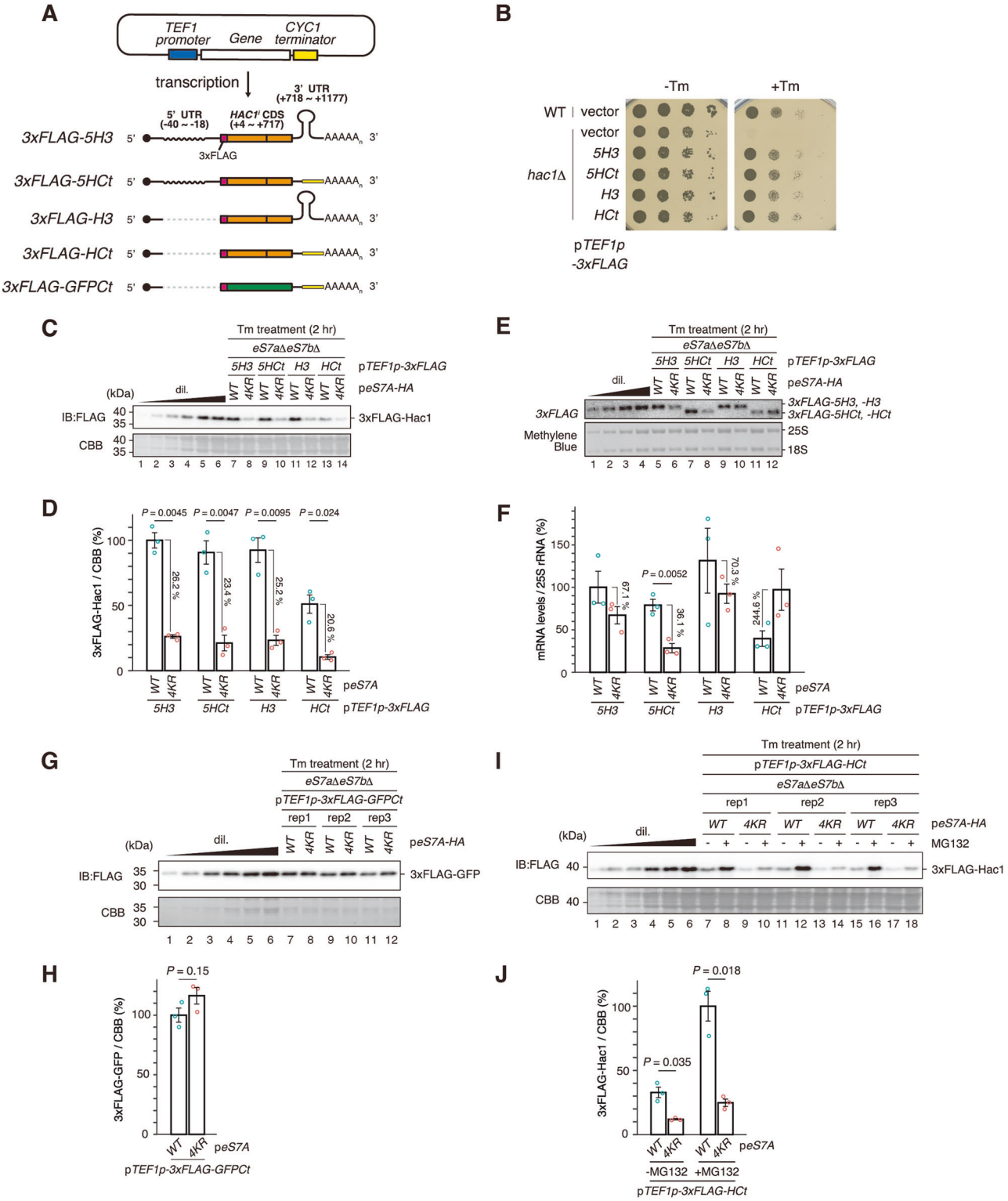

the LRR domain is required for regulation but not interaction. Grr1 interacts with Ubp3 independent of Tm treatment (Fig. 2); however, the downregulation of Ubp3 by Grr1 only under Tm treatment conditions (Fig. 1) indicates that Grr1-mediated degradation of Ubp3 under stress conditions requires unknown regulation to induce Ubp3 degradation after interaction with E3 ligase. Ubp3 roles in quality controls, indicating that the deubiquitination is a key reaction to ensure the accuracy of gene express[21,23–25,27,28]. The results of this study revealed the crucial role of ubiquitin-proteasomal degradation of the deubiquitinating enzyme under stress conditions in maintaining translation of transcription factor Hac1 in yeast. We have observed that F-box and LRR domains are required for Ubp3 destabilization by Tm treatment (Fig. 2D and Supplementary Fig. 4) and normal growth (Fig. 2E). Grr1 associates with core SCF to form the SCF^{Grr1} complex. The CLN1/2 and GIC2 are well-characterized substrate of the SCF^{Grr1} complex and required for the G1/S cell cycle transition. Therefore, we suspect that F-box and LRR domains are required for CLN1/2 and GIC2 and the G1/S cell cycle transition.

The mechanisms underlying the role of eS7A ubiquitination in the translational regulation of ER stress remains unknown. Ribosome

Fig. 6 | UTRs of *HAC1* are not the target for eS7A ubiquitination-mediated translational regulation. A Schematic drawing of *3xFLAG-HAC1*^{i} and *3xFLAG-GFP* mRNAs. **B** Tunicamycin sensitivity of *hac1*Δ cells expressing *3xFLAG-HAC1*^{i} reporters. 10-fold serial dilutions of the indicated cells were spotted onto the plates. Plates were incubated at 30 °C for 2–3 days. **C** 3xFLAG-Hac1p expression is increased by eS7A ubiquitination independent of UTRs of *HAC1*. Yeast cells harboring plasmids encoding *3xFLAG-HAC1*^{i} shown in (**A**) under the control of *TEF1* promoters were harvested as in Fig. 1B. The samples were analyzed using western blotting with anti-FLAG antibody. CBB staining was used as a loading control. Dilutions are 100%, 75%, 50%, 25%, 12.5%, 6.25%. **D** The 3xFLAG-Hac1p/CBB levels shown in (**C**) and Supplementary Fig. 8D were quantified and normalized relative to that from *eS7A(WT)* expressing *3xFLAG-5H3*. The percentages indicate the protein levels ratio in *eS7A(4KR)* to that in *eS7A(WT)*. **E** *3xFLAG-HAC1*^{i} mRNA levels in *eS7A(WT)* and *eS7A(4KR)*. Yeast cells were harvested, and the samples were analyzed as in Fig. 5G, using DIG-labeled *3xFLAG* probe. **F** *3xFLAG-HAC1*^{i} mRNA/25S rRNA levels shown in (**E**) and Supplementary Fig. 8E were quantified and normalized as in (**D**). **G** 3xFLAG-GFP expressions are almost the same between *eS7A(WT)* and *eS7A(4KR)*. Yeast cells expressing *3xFLAG-GFPCt* by *TEF1* promoters were harvested, and the samples were analyzed as in (**C**). **H** The 3xFLAG-GFP/CBB levels shown in (**G**) were quantified and normalized relative to that from *eS7A(WT)*. **I** Proteasome-dependent degradation of 3xFLAG-Hac1p in *eS7A(WT)* and *eS7A(4KR)*. Yeast cells harboring plasmids encoding *3xFLAG-HCt* under control of *TEF1* promoter were grown at 30 °C until OD_{600} = 0.2, then treated with 1 μg/mL of Tm and 50 μM of MG132 for 2 h and harvested. The samples were analyzed as in (**C**). **J** The 3xFLAG-Hac1p/CBB levels shown in (**I**) were quantified and normalized relative to that in *eS7A(WT)* with 50 μM MG132 treatment. All experiments were repeated at least twice with biologically independent samples and showed similar results. Data represent $n = 3$ biologically independent experiments (mean ± SE), and *P*-values were calculated by Two-sided Welch's t-test. Source data are provided as a Source Data file.

profiling revealed that *HAC1*^{i} was the most significantly upregulated gene during the UPR (Fig. 4). Translation of *HAC1*^{i} mRNA was significantly lower in *eS7-4KR* cells[18] and *grr1*Δ cells than in wild-type cells (Fig. 4). One possibility is that eS7A ubiquitination affects the interaction between the 40S subunit and translation initiation factors in the pre-initiation complex, thereby modulating the translation initiation of *HAC1*^{i} mRNA. The cycle of ubiquitination and deubiquitination of the 40S ribosomal subunit, eS7A, is important for efficient translation[19,20]. The two deubiquitinating enzymes, Otu2 and Ubp3, for eS7A cause defects in protein synthesis[19,20]. Otu2 specifically binds to free 40S ribosomes and promotes the dissociation of mRNAs from 40S ribosomes during recycling. Despite the crucial role of Otu2 in translation initiation, the *otu2*Δ mutant was resistant to Tm[20]. Ubp3 inhibited the polyubiquitination of eS7A in polysomes to maintain eS7A in a mono-ubiquitinated form, however, *otu2*Δ suppressed moderate sensitivity of the *ubp3*Δ mutant to Tm (Supplementary Fig. 10). The *otu2* mutation that disrupts the deubiquitinating activity of Otu2 could not rescue the Tm resistance of *ubp3*Δ*otu2*Δ cells, suggesting that this suppression depends on the lack of the deubiquitinating activity of Otu2 (Supplementary Fig. 10). These suggest that translation initiation may be involved but not crucial for *HAC1*^{i} translation.

We observed that eS7A ubiquitination is essential for the translation of *HAC1*^{i} mRNA, which lacks 5′ UTR, 3′ UTR, and introns, even under normal conditions (Figs. 5–7). This suggests that the ORF of *HAC1*^{i} mRNA contains elements required for eS7A ubiquitination-mediated regulation, and eS7A ubiquitination facilitates the translation elongation of *HAC1*^{i} mRNA. Together with the previous footprints of *eS7A-WT* and *eS7A-4KR* also revealing putative translation pausing sites, we propose that eS7A ubiquitination facilitates the translation elongation of *HAC1*^{i} mRNA depending on the cis-element in ORF (Fig. 7I). Given that Ubp3 deubiquitinates the ribosomal protein eS7A in the 80S and polysome fractions, the maintenance of eS7A ubiquitination in translating ribosomes could contribute to the efficient translation elongation of *HAC1*^{i} mRNA.

The Ccr4-NOT complex monitors translating ribosomes for codon optimality via E-site binding of the N-terminal domain of the Not5 subunit[17]. eS7A ubiquitination contributes to the interaction of the Ccr4-Not complex with the ribosome, and thereby codon-optimality-mediated mRNA degradation. The phenotypes of Not4 deletion or the eS7A-4KR mutation were hardly aggravated by additional deletion of Not5-NTD but reduced Not5 association with polyribosomes[17], suggesting that eS7A-ubiquitination by Not4 is involved in the same pathway as Not5 but occurs upstream of E-site probing, and Not5 binding to ribosomes is dependent on prior eS7A-ubiquitination. Our results suggest that Not4-mediated eS7A ubiquitination is required for the efficient translation elongation of *HAC1*^{i} mRNA. Although the Ccr4-Not complex association with ribosomes is required for codon optimality-mediated mRNA decay, the stability of the 50% optimal *HIS3* reporter mRNA was not changed in the *eS7A-4KR* or *not5*Δ mutant cells[17]. The codon optimality of *HAC1*^{i} mRNA is 50%, and its mRNA level did not decrease in the *eS7A-4KR* mutant cells[18]. More importantly, *GFP*, with the same codon optimality as *HAC1*^{i} mRNA in yeast, can suppress eS7A-mediated regulation. Taken together, we suspect that codon optimality is not solely responsible for the regulation of *HAC1*^{i} translation. In mammalian cells, the secondary structure of mRNA contributes to translation and possibly mRNA stability, although its mechanism remains unknown. A more precise analysis of the cis-elements in *HAC1*^{i} mRNA and the involvement of trans factors, including Ccr4-NOT, is needed to elucidate the mechanisms underlying the eS7A ubiquitination-mediated regulation of *HAC1*^{i} mRNA translation elongation. Further experiments will shed light on how eS7A ubiquitination stimulates the translation of *HAC1*^{i} mRNA, providing insight into the crucial role of ribosome ubiquitination in stress responses in addition to well-characterized roles in translation quality controls.

In this study, we also analyzed the transcription and splicing of *HAC1* mRNA. The statistical analysis of the results indicates that no statistically significant difference in *HAC1* mRNA levels between wild-type (WT) and *grr1*Δ mutant cells (Fig. 5K and Supplementary Fig. 1C, D). In contrast, Grr1 facilitates the splicing of *HAC1*^{u} mRNA (Supplementary Fig. 1B–E). The splicing of *HAC1*^{u} mRNA does not change in the *eS7A-4KR* and the *ubp3*Δ mutant cells[18]. We propose that Grr1 regulates *HAC1*^{u} mRNA splicing independently of Ubp3 and eS7A ubiquitination. Further analysis will uncover the Grr1 function in the co-localization and *HAC1* mRNA and Ire1 protein on the ER membrane required for *HAC1*^{u} mRNA splicing. Given that Grr1-mediated Ubp3 degradation is crucial for maintaining eS7A ubiquitination during UPR, we propose that Grr1 facilitates the splicing of *HAC1*^{u} mRNA independently of Ubp3 and eS7A ubiquitination, as well as the translation of *HAC1*^{i} mRNA in a Ubp3- and ubiquitination of eS7A-dependent manner (Fig. 7I). Further investigation into how Grr1 facilitates *HAC1*^{u} mRNA splicing and translation of *HAC1*^{i} mRNA depending on the cis-element in ORF.

Methods

Yeast strains and genetic methods

The *Saccharomyces cerevisiae* strains used in this study are listed in Supplementary Data 1. Yeast Knock Out (YKO) library strains (BY4741) (Open Biosystems) used in E3 ligase screening are indicated in Supplementary Fig. 1A. Gene disruption, C-terminal tagging and N-terminal tagging were performed following previously reported methods[52–54]. Yeast *Saccharomyces cerevisiae* W303-1a based strains were obtained by established recombination techniques using PCR-amplified cassette sequences (*kanMX4*, *hphMX4*, *hphNT1*, *natMX4*, or *HISMX6*). To construct strains of essential ribosomal protein genes, the shuffle strains transformed with plasmids expressing mutant ribosomal protein products were grown on SDC plate containing 0.1%(w/v) of 5-fluoroorotic acid (5-FOA, #F9001-5, Zymo Research) and isolated *URA3* absent strains.

https://doi.org/10.1038/s41467-025-57360-1

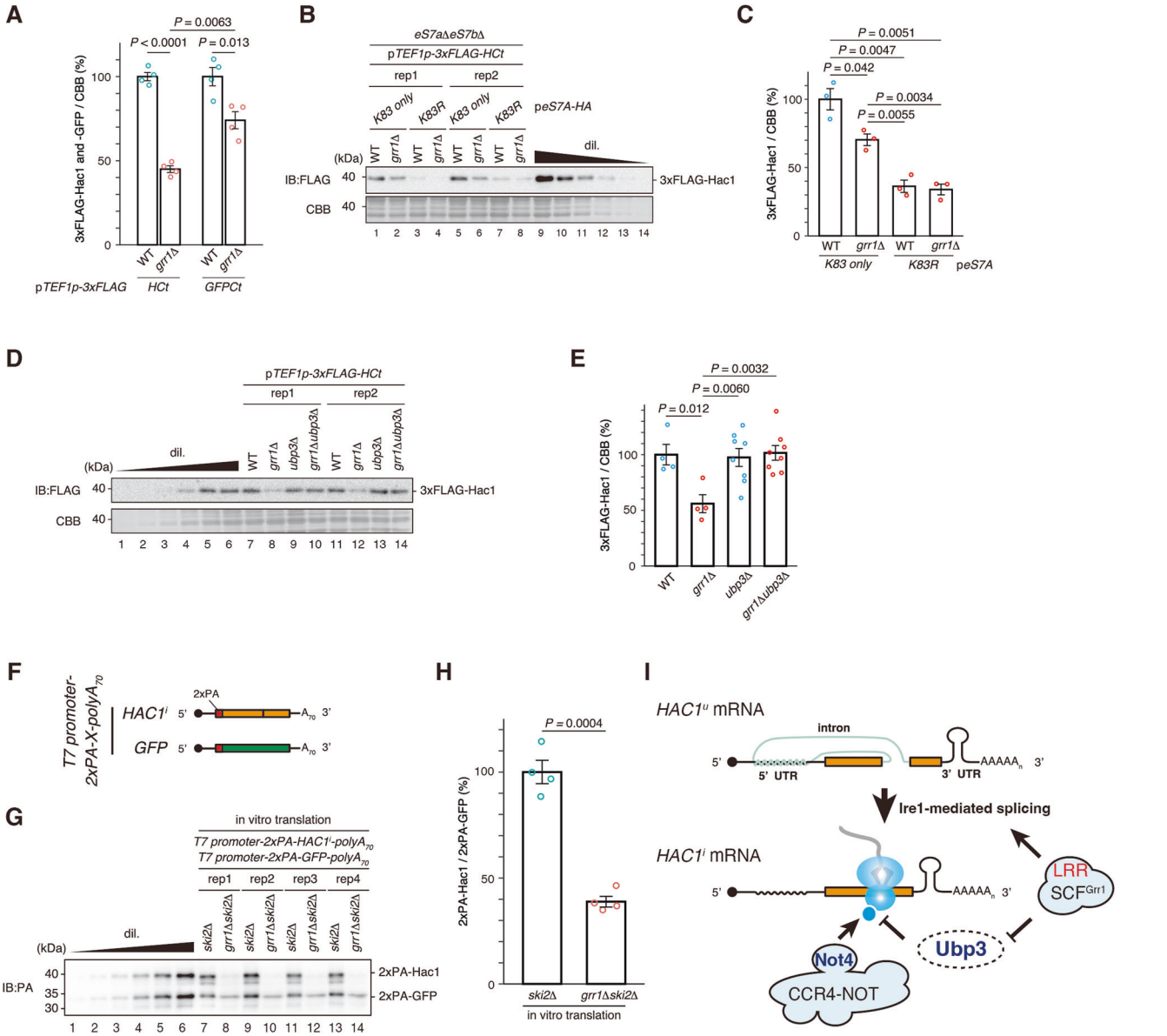

Fig. 7 | Grr1 is involved in efficient *HAC1*^{i} translation via eS7A ubiquitination. **A** 3xFLAG-Hac1p/CBB and 3xFLAG-GFP/CBB levels shown in Supplementary Fig. 9A were quantified and normalized protein levels relative to that in WT. **B** 3xFLAG-Hac1p expressions are decreased in *grr1ΔeS7A(K83 only), eS7A(K83R)* and *grr1ΔeS7A(K83R)*. Yeast cells harboring plasmids encoding *3xFLAG-HCt* under control of *TEF1* promoters were grown at 30 °C and harvested at log phase. The samples were analyzed using western blotting with anti-FLAG antibody. CBB staining was used as a loading control. Dilutions are 100%, 75%, 50%, 25%, 12.5%, 6.25%. **C** 3xFLAG-Hac1p/CBB levels shown in (**B**) and Supplementary Fig. 9B were quantified and normalized protein levels relative to that in *eS7A(K83 only)*. Data represent $n = 3$ biologically independent experiments (mean ± SE). **D** 3xFLAG-Hac1p expressions are decreased in *grr1*Δ, but not in *grr1*Δ*ubp3*Δ. Yeast cells harboring plasmids encoding *3xFLAG-HCt* under control of *TEF1* promoters were grown at 30°C and harvested at log phase. The samples were analyzed as in (**B**). **E** 3xFLAG- Hac1p/CBB levels shown in (**D**) and Supplementary Fig. 9C were quantified and normalized protein levels relative to that in WT. Data represent $n = 4$ (WT, *grr1*Δ) or 8 (*ubp3*Δ, *grr1*Δ*ubp3*Δ) biologically independent experiments (mean ± SE). **F** Schematic drawings of *T7 promoter–2xPA-(HAC1*^{i} or *GFP)-polyA*$_{70}$ mRNAs. **G** 2xPA-Hac1 translation is decreased in *grr1*Δ*ski2*Δ lysate. In vitro translation was performed using *2xPA-HAC1*^{i}*-polyA*$_{70}$ and *2xPA-GFP-polyA*$_{70}$ mRNAs at 17 °C for 30 min. The samples were analyzed using western blotting with anti-PA antibody. Dilutions are 100%, 75%, 50%, 25%, 12.5%, 6.25%. **H** 2xPA-Hac1/2xPA-GFP levels shown in (**G**) were quantified and normalized protein levels relative to that in *ski2*Δ lysate. **I** Model for the crucial role of Grr1-mediated degradation of Ubp3 in the translation of *HAC1*^{i} mRNA. Not4-mediated mono-ubiquitination of eS7A is required for efficient translation of *HAC1*^{i} mRNA. The SCF^{Grr1} complex is responsible for the downregulation of Ubp3, which facilitates eS7A ubiquitination and *HAC1*^{i} translation. All experiments were repeated at least twice with biologically independent samples and showed similar results. Data in (**A**, **H**) represent $n = 4$ biologically independent experiments (mean ± SE). *P* values were calculated by Two-sided Welch's t-test. Source data are provided as a Source Data file.

Plasmid constructs

DNA cloning was performed with PCR amplification by using gene specific primers and KOD FX Neo (#KFX-201, TOYOBO), and by using T4 DNA ligase (#M0202S, NEB). All cloned DNAs amplified by PCR were verified by sequencing. Plasmids used in this study are listed in Supplementary Data 2. Sequences used in Figs. 6 and 7 are listed in Supplementary Data 3. These plasmids contain part of an *ARS*, part of a *CEN* and *CYC1* terminator.

Yeast culture and media

All yeast cells were cultured with YPD or synthetic complete (SC) medium with 2% glucose at 30 °C and harvested by centrifugation and

discarding medium. To induce ER stress, yeast cells were grown at 30 °C until OD_{600} = 0.2, then treated with 1 μg/mL of tunicamycin (Tm, #208-08243, Wako) for ~4 h and harvested. A proteasome inhibitor MG132 (#HY-13259, MCH) was added with tunicamycin to a final concentration of 50 μM. All cell pellets were frozen in liquid nitrogen immediately after harvest and stored at −80 °C until used.

RNA isolation, RNA electrophoresis and northern blotting

Yeast cells were harvested at indicated time points (~ 4 h) after Tm added, as described above. Total RNA solutions were prepared by using one-step hot formamide RNA extraction method and RNA electrophoresis was performed as described[55,56]. Yeast cell pellet in 1.5 mL tube (stand on ice) was resuspended with 50 μL of FAE solution and heated at 70 °C for 10 min. After centrifugation at 17,800 x g for 1 min at room temperature, 40 μL of the supernatant containing total RNA was collected. RNA samples containing 1.2 μg of total RNA were incubated at 70 °C for 5 min and left to stand on ice for 10 min. Each sample was electrophoresed at 200 V for 50 min on a 1.2% HT-FA agarose gel in HT buffer, followed by transfer of RNA to Hybond-N+ membrane (GE healthcare) with 20x SSC for over 18 h using capillary system. RNA was cross-linked on the membrane by CL-1000 ultraviolet crosslinker (UVP) at 120 mJ/cm^2. Membrane was incubated with DIG Easy Hyb Granules (#11796895001, Roche) for 1 h at 50 °C in a hybridization oven and DIG-labelled probe prepared using PCR DIG Probe Synthesis Kit (#11636090910, Roche) was added and incubated for over 18 h. The membrane was washed with wash buffer I for 15 min in a hybridization oven, followed by washing twice with wash buffer II for 15 min in a hybridization oven. The membrane was then washed with 1x maleic acid buffer for 10 min at room temperature and incubated with Blocking Reagent (#11096176001, Roche) for 30 min. Anti-Digoxigenin-AP, Fab fragments (#11093274910, Roche) was added to the Blocking Reagent and the membrane was further incubated for 1 h. After that, the membrane was washed three times with wash buffer III for 10 min and equilibrated by equilibration buffer. The membrane was reacted with CDP-star (#11759051001, Roche) for 10 min, and chemiluminescence was detected by LAS-4000 (GE healthcare). Quantification of band intensities were performed using ImageQuant TL software (Cytiva).

- FAE solution (98% deionized Formamide, 10 mM EDTA)
- RNA sample (50% deionized Formamide, 30 mM HEPES, 30 mM Triethanolamine, 0.4 M Formaldehyde (#061-00416, Wako), 0.5 mM EDTA, 0.02% bromophenol blue)
- HT buffer (30 mM HEPES, 30 mM Triethanolamine)
- 1.2% HT-FA agarose gel (Agarose LE Analytical Grade (#V3125, Promega), 30 mM HEPES, 30 mM Triethanolamine, 0.4 M Formaldehyde)
- 20x SSC (3 M NaCl, 300 mM Trisodium citrate dihydrate)
- Wash buffer I (2x SSC, 0.1% SDS)
- Wash buffer II (0.1x SSC, 0.1% SDS)
- 1x maleic acid buffer (100 mM maleic acid, 150 mM NaCl, pH 7.0, adjusted by NaOH)
- Wash buffer III (1x maleic acid buffer, 0.3% tween 20)
- Equilibration buffer (100 mM Tris-HCl pH 9.4, 100 mM NaCl)

Trichloroacetic acid (TCA) precipitation for protein preparation

Yeast cell pellet in 1.5 mL tube (stand on ice) was resuspended with 1 mL of ice-cold double-distilled water containing 1 mM phenylmethylsulfonyl fluoride (PMSF, #164-12181, Wako). 100 μL of yeast suspension was diluted with 900 μL of double-distilled water followed by OD_{600} measurement. To the rest of yeast suspension (900 μL), 135 μL of Lysis buffer was added and incubated on ice for 15 min. After that, 135 μL of 50% TCA was added to samples and incubated on ice for 10 min. After centrifugation of lysates (17,800 x g, 10 min, 4 °C), the supernatant was discarded completely, and the pellet was dissolved in HU buffer (250 μL/OD_{600}) and heated at 65 °C for 10 min. After centrifugation at 17,800 x g for 5 min at room temperature, the supernatant was used as a sample for SDS-PAGE.

- Lysis buffer (2 M NaOH, 1 M 2-Mercaptoethanol)
- HU buffer (8 M Urea, 200 mM Tris-HCl pH 6.8, 5% SDS, 1 mM EDTA, 0.01% BPB, 100 mM DTT)

Protein electrophoresis and western blotting

Protein samples were separated by SDS-PAGE, and were transferred onto PVDF membrane (Immobilon-P, Millipore). After blocking with 5% skim milk in PBS-T, the membrane was incubated with primary antibodies overnight at 4 °C. The membrane was washed with PBS-T for three times followed by incubation with horseradish peroxidase (HRP)-conjugated secondary antibodies for 1 h at room temperature. In the case of HA-tagged protein detection, the membrane was incubated with HRP-conjugated anti-HA antibodies. After washing with PBS-T for three times, chemiluminescence was detected by LAS4000 (GE Healthcare) or Amersham ImageQuant 800 (Cytiva). Primary antibodies for western blotting in this study were listed in Supplementary Data 4. Quantification of band intensities were performed using ImageQuant TL software (Cytiva) and Multi Gauge software (Fuji film).

- PBS-T (10 mM Na2HPO4/NaH2PO4 pH 7.5, 0.9% NaCl, 0.1% Tween-20)

Spot assay

Yeast cells were cultured with 3 mL YPD or SC medium with 2% glucose at 30 °C overnight and adjusted to OD_{600} = 0.3. 10-fold serial dilutions were prepared in the 1.5 mL tubes and spotted onto 1 μg/mL Tm added plates and control plates. Plates were incubated at 30 °C for several days.

Ribosome Profiling (Ribo-seq) and RNA-seq

Library preparation was performed as described[18] with following modifications. After 4 h of tunicamycin treatment, yeast cells were harvested by filtration and frozen by liquid nitrogen. They were lysed by lysis buffer for Ribo-seq (20 mM Tris-HCl pH 7.5, 150 mM NaCl, 5 mM $MgCl_2$, 1 mM DTT, 1% Triton X-100, 0.1 mg/mL cycloheximide, 25 U/mL Turbo DNase (Invitrogen, AM2238)). Clear lysates were obtained by centrifugation at 20,000 x g for 10 min at 4 °C. Clear lysate containing 20 μg total RNA was treated with 1.25 unit of RNase I (#E0067-10D1, LGC Biosearch Technologies) per μg RNA for 45 min at 25 °C. RNase I treatment was quenched by the addition of 200 units of SUPERase· In RNase Inhibitor (Invitrogen, AM2694). RNA-digested lysate was layered on a sucrose cushion (1 M sucrose, 20 mM Tris-HCl pH 7.5, 150 mM NaCl, 5 mM $MgCl_2$, 1 mM DTT, 0.1 mg/mL cycloheximide, 20 U/mL SUPERase· In RNase Inhibitor), followed by centrifugation in a TLA-110 rotor (Beckman) at 542,715 x g for 1 h at 4 °C. The ribosomal pellet was resuspended in 120 μL of splitting buffer (20 mM Tris-HCl pH 7.5, 300 mM NaCl, 5 mM EDTA, 1% Triton X-100, 1 mM DTT, 20 U/mL of SUPERase· In RNase Inhibitor) to dissociate ribosomes from the mRNA fragments, and then passed through the 100 kDa MWCO Amicon Ultra-0.5 device (Millipore, UFC5100). The non-ribosomal flow-through (approximately 100 μL) was collected and mixed with 300 μL TRIzol reagent (Invitrogen, 15596018). RNA fragments were extracted by Direct-zol RNA MicroPrep (Zymo Research). For the ribosome profiling analysis, the whole cell lysate containing 20 μg of total RNA was treated with 1.25 units/1 μg RNA of RNase I (#E0067-10D1, LGC Biosearch Technologies) at 25 °C for 45 min. As linker DNA, 5′-(Phos)NNNNNIIIIITGATCGGAAGAGCACACGTCTGAA(ddC)-3′ where (Phos) indicated 5′ phosphorylation and (ddC) indicates a terminal 2′, 3′-dideoxycytidine, was used. The Ns and Is indicate random barcodes for eliminating PCR duplication and multiplexing barcodes, respectively. The linkers were pre-adenylated with 5′ DNA Adenylation kit (NEB), and then used for the ligation reaction. The rRNAs were removed using a mixture of riboPOOL (siTOOLs Biotech) and homemade customized biotinylated oligos. An oligo 5′-(Phos)

NNAGATCGGAAGAGCGTCGTGTAGGGAAAGAG(iSp18)GTGACTGGA GTTCAGACGTGTGCTC-3', where (Phos) indicated 5' phosphorylation and Ns indicate random barcode, was used for reverse transcription. PCR was performed with oligos, 5'-AATGATACGGCGACCACCGA-GATCTACACTCTTTCCCTACACGACGCTC-3' and 5'- CAAGCAGAAGAC GGCATACGAGATJJJJJJGTGACTGGAGTTCAGACGTGTG-3', where Js indicate reverse complement of the index sequence discovered during Illumina sequencing. The libraries were sequenced on a HiSeq X Ten (Illumina) at Macrogen Japan corp.

For the RNA-seq analysis, total RNA was extracted from lysate using Direct-zol RNA Microprep w/ Zymo-Spin IC Columns (#R2062, funakoshi). The libraries were sequenced on a DNBSEQ-G400RS High-throughput Sequencing Kit (MGI Tech Co., Ltd.) at Bioengineering Lab, Japan. The reads were mapped to yeast transcriptome, removing duplicated reads based on random barcode sequences. The analyzes for ribosome profiling were restricted to 27-29 nt reads for WT and *grr1*Δ data sets. The DESeq2 package was used to calculate the fold change of mRNA expression and translation efficiency (TE).

Cycloheximide chase assay

To analyze the Ubp3-3HA stability, yeast cells were treated with 0.25 mg/mL cycloheximide after 1 h of tunicamycin treatment. At the indicated time points, yeast cells were treated with 30 mM sodium azide and harvested by centrifugation and discarding medium. A proteasome inhibitor MG132 (#HY-13259, MCH) was added simultaneously with tunicamycin to a final concentration of 50 μM. To analyze the 3xFLAG-Hac1p stability, yeast cells were treated with tunicamycin for 2 h, then harvested by centrifugation and discarding medium, and resuspended in 6 mL of SDC medium with 1 μg/mL tunicamycin and incubated at 30 °C for 5 min. As 0 min samples, 1.4 mL of yeast cell cultures were treated with 30 mM sodium azide and harvested by quick centrifugation. Then yeast cells were treated with 0.25 mg/mL cycloheximide and 1 mL of yeast cell cultures were treated with 30 mM sodium azide and harvested by quick centrifugation at indicated time points. Protein stability was determined by western blotting.

Immunoprecipitation using FLAG beads

After 1.5 h of tunicamycin treatment, then yeast cells were harvested by centrifugation (8983 x g, 5 min, room temperature) and discarding medium. All cell pellets were frozen in liquid nitrogen immediately after harvest and stored at −80 °C until used. After grinding the cell pellets in liquid nitrogen with a mortar and a pestle, the cell pellets were lysed with Lysis buffer for IP to prepare crude lysate. Anti DYKDDDDK tag Antibody Beads (# 016-22784, Wako) were added to the crude lysate and rotated at 4 °C for 1 h. The beads were washed 7 times with Wash buffer for IP. FLAG-tagged proteins were eluted twice by Elution buffer for IP with FLAG peptide at 4 °C for 1 h. After TCA precipitation, samples were subjected to SDS-PAGE and western blotting.

- Lysis buffer for IP (50 mM Tris-HCl pH 7.5, 100 mM NaCl, 10 mM $MgCl_2$, 2 mM 2-Mercaptoethanol, 0.01% NP-40, 1 tablet/10 mL cOmplete mini EDTA-free (# 11836170001, Roche))
- Wash buffer for IP (50 mM Tris-HCl pH 7.5, 100 mM NaCl, 10 mM $MgCl_2$, 2 mM 2-Mercaptoethanol, 0.01% NP-40)
- Elution buffer for IP with FLAG peptide (50 mM Tris-HCl pH 7.5, 100 mM NaCl, 10 mM $MgCl_2$, 2 mM 2-Mercaptoethanol, 0.01% NP-40, 100 μg/mL FLAG® Peptide (# F3290, Sigma aldrich))

In vitro translation

In vitro translation was performed as describe[7] with following modifications. Reporter mRNAs was produced using the mMessage mMachine Kit (Thermo Fischer) and the sequences were listed in Supplementary Data 3. To prepare yeast cell-free translation extract, yeast cells were grown in YPD medium to an OD_{600} of 1.5–2.0, then washed with water and 100 mM KCl, and finally incubated with 10 mM DTT in 100 mM Tris-HCl pH 8.0 for 15 min at room temperature. After centrifugation, cells were resuspended in YPD/1 M sorbitol (3.3 mL per 1 g of cell pellet). To generate spheroplasts, 2.69 mg zymolyase per 1 g of cell pellet was added to cells and incubated for 90 min at 30 °C. Spheroplasts were then washed three times with YPD/1 M sorbitol and once with 1 M sorbitol, and lysed with a douncer in lysis buffer for IVT. From the lysate, an S100 fraction was obtained by low-speed centrifugation followed by ultracentrifugation of the supernatant. The S100 was passed through a PD10 column (Cytiva). In vitro translation was performed at 17 °C for 30 min using a large excess of template mRNA (2 μg per 20 μL of extract), and stopped by mixing with a quarter volume of 4xSB (final 1xSB) and flash frozen in liquid nitrogen. Samples were thawed and heated at 95 °C for 5 min. After centrifugation at 17,800 x g for 5 min at room temperature, the supernatant was used as a sample for SDS-PAGE.

- Lysis buffer for IVT (20 mM HEPES-KOH pH 7.5, 100 mM KOAc, 2 mM Mg(OAc)2, 10% Glycerol, 1 mM DTT, 0.5 mM PMSF, 1 tablet/10 mL cOmplete mini EDTA-free)
- 4xSB (200 mM Tris-HCl pH 6.8, 8% SDS, 40% Glycerol, 0.04% BPB, 100 mM DTT)

Statistics and reproducibility

In Fig. 4, Q values were calculated by Two-sided Likelihood ratio test. For other statistical analyses, *P* values were calculated by Two-sided Welch's t-test. All experiments were repeated at least twice with biologically independent samples.

Reporting summary

Further information on research design is available in the Nature Portfolio Reporting Summary linked to this article.

Data availability

The sequencing data of RNA-seq and ribosome profiling have been deposited in the NCBI Gene Expression Omnibus and are accessible through GEO series accession number GSE260735 (RNA-seq) and GSE260736 (Ribo-seq), respectively. Source data are provided with this paper.

References

1. Joazeiro, C. A. P. Mechanisms and functions of ribosome-associated protein quality control. *Nat. Rev. Mol. Cell Biol.* **20**, 368–383 (2019).
2. Monaghan, L., Longman, D. & Cáceres, J. F. Translation-coupled mRNA quality control mechanisms. *Embo J.* **42**, e114378 (2023).
3. Brandman, O. & Hegde, R. S. Ribosome-associated protein quality control. *Nat. Struct. Mol. Biol.* **23**, 7–15 (2016).
4. Shao, S. & Hegde, R. S. Target Selection during Protein Quality Control. *Trends Biochem Sci.* **41**, 124–137 (2016).
5. Inada, T. Quality controls induced by aberrant translation. *Nucleic Acids Res* **48**, 1084–1096 (2020).
6. Narita, M. et al. A distinct mammalian disome collision interface harbors K63-linked polyubiquitination of uS10 to trigger hRQT-mediated subunit dissociation. *Nat. Commun.* **13**, 6411 (2022).
7. Matsuo, Y., Uchihashi, T. & Inada, T. Decoding of the ubiquitin code for clearance of colliding ribosomes by the RQT complex. *Nat. Commun.* **14**, 79 (2023).
8. Matsuo, Y. et al. Ubiquitination of stalled ribosome triggers ribosome-associated quality control. *Nat. Commun.* **8**, 159 (2017).
9. Ikeuchi, K. et al. Collided ribosomes form a unique structural interface to induce Hel2-driven quality control pathways. *Embo J.* **38** https://doi.org/10.15252/embj.2018100276 (2019).
10. Best, K. et al. Structural basis for clearing of ribosome collisions by the RQT complex. *Nat. Commun.* **14**, 921 (2023).
11. Matsuo, Y. et al. RQT complex dissociates ribosomes collided on endogenous RQC substrate SDD1. *Nat. Struct. Mol. Biol.* **27**, 323–332 (2020).

12. Hashimoto, S., Sugiyama, T., Yamazaki, R., Nobuta, R. & Inada, T. Identification of a novel trigger complex that facilitates ribosome-associated quality control in mammalian cells. *Sci. Rep.* **10**, 3422 (2020).
13. D'Orazio, K. N. et al. The endonuclease Cue2 cleaves mRNAs at stalled ribosomes during No Go Decay. *Elife* **8** https://doi.org/10.7554/eLife.49117 (2019).
14. Tomomatsu, S. et al. Two modes of Cue2-mediated mRNA cleavage with distinct substrate recognition initiate no-go decay. *Nucleic Acids Res* **51**, 253–270 (2023).
15. Collart, M. A. Global control of gene expression in yeast by the Ccr4-Not complex. *Gene* **313**, 1–16 (2003).
16. Collart, M. A. The Ccr4-Not complex is a key regulator of eukaryotic gene expression. *Wiley Interdiscip Rev. RNA* https://doi.org/10.1002/wrna.1332 (2016).
17. Buschauer, R. et al. The Ccr4-Not complex monitors the translating ribosome for codon optimality. *Science* **368** https://doi.org/10.1126/science.aay6912 (2020).
18. Matsuki, Y. et al. Ribosomal protein S7 ubiquitination during ER stress in yeast is associated with selective mRNA translation and stress outcome. *Sci. Rep.* **10**, 19669 (2020).
19. Takehara, Y. et al. The ubiquitination-deubiquitination cycle on the ribosomal protein eS7A is crucial for efficient translation. *iScience* **24**, 102145 (2021).
20. Ikeuchi, K. et al. Molecular basis for recognition and deubiquitination of 40S ribosomes by Otu2. *Nat. Commun.* **14**, 2730 (2023).
21. Fang, N. N., Zhu, M., Rose, A., Wu, K. P. & Mayor, T. Deubiquitinase activity is required for the proteasomal degradation of misfolded cytosolic proteins upon heat-stress. *Nat. Commun.* **7**, 12907 (2016).
22. Jung, Y. et al. Modulating cellular balance of Rps3 mono-ubiquitination by both Hel2 E3 ligase and Ubp3 deubiquitinase regulates protein quality control. *Exp. Mol. Med* **49**, e390 (2017).
23. Kraft, C., Deplazes, A., Sohrmann, M. & Peter, M. Mature ribosomes are selectively degraded upon starvation by an autophagy pathway requiring the Ubp3p/Bre5p ubiquitin protease. *Nat. Cell Biol.* **10**, 602–610 (2008).
24. Kraft, C. & Peter, M. Is the Rsp5 ubiquitin ligase involved in the regulation of ribophagy? *Autophagy* **4**, 838–840 (2008).
25. Kvint, K. et al. Reversal of RNA polymerase II ubiquitylation by the ubiquitin protease Ubp3. *Mol. Cell* **30**, 498–506 (2008).
26. Oling, D., Masoom, R. & Kvint, K. Loss of Ubp3 increases silencing, decreases unequal recombination in rDNA, and shortens the replicative life span in Saccharomyces cerevisiae. *Mol. Biol. Cell* **25**, 1916–1924 (2014).
27. Ossareh-Nazari, B. et al. Cdc48 and Ufd3, new partners of the ubiquitin protease Ubp3, are required for ribophagy. *EMBO Rep.* **11**, 548–554 (2010).
28. Ossareh-Nazari, B. et al. Ubiquitylation by the Ltn1 E3 ligase protects 60S ribosomes from starvation-induced selective autophagy. *J. Cell Biol.* **204**, 909–917 (2014).
29. Ron, D. & Walter, P. Signal integration in the endoplasmic reticulum unfolded protein response. *Nat. Rev. Mol. Cell Biol.* **8**, 519–529 (2007).
30. Walter, P. & Ron, D. The unfolded protein response: from stress pathway to homeostatic regulation. *Science* **334**, 1081–1086 (2011).
31. Xu, C., Bailly-Maitre, B. & Reed, J. C. Endoplasmic reticulum stress: cell life and death decisions. *J. Clin. Invest* **115**, 2656–2664 (2005).
32. Cox, J. S. & Walter, P. A novel mechanism for regulating activity of a transcription factor that controls the unfolded protein response. *Cell* **87**, 391–404 (1996).
33. Willems, A. R. et al. SCF ubiquitin protein ligases and phosphorylation-dependent proteolysis. *Philos. Trans. R. Soc. Lond. B Biol. Sci.* **354**, 1533–1550 (1999).
34. Rüegsegger, U., Leber, J. H. & Walter, P. Block of HAC1 mRNA translation by long-range base pairing is released by cytoplasmic splicing upon induction of the unfolded protein response. *Cell* **107**, 103–114 (2001).
35. Cox, J. S., Shamu, C. E. & Walter, P. Transcriptional induction of genes encoding endoplasmic reticulum resident proteins requires a transmembrane protein kinase. *Cell* **73**, 1197–1206 (1993).
36. Tirasophon, W., Welihinda, A. A. & Kaufman, R. J. A stress response pathway from the endoplasmic reticulum to the nucleus requires a novel bifunctional protein kinase/endoribonuclease (Ire1p) in mammalian cells. *Genes Dev.* **12**, 1812–1824 (1998).
37. Higgins, R. et al. The Unfolded Protein Response Triggers Site-Specific Regulatory Ubiquitylation of 40S Ribosomal Proteins. *Mol. Cell* **59**, 35–49 (2015).
38. Flick, J. S. & Johnston, M. GRR1 of Saccharomyces cerevisiae is required for glucose repression and encodes a protein with leucine-rich repeats. *Mol. Cell Biol.* **11**, 5101–5112 (1991).
39. Skowyra, D. et al. Reconstitution of G1 cyclin ubiquitination with complexes containing SCFGrr1 and Rbx1. *Science* **284**, 662–665 (1999).
40. Kusama, K. et al. Dot6/Tod6 degradation fine-tunes the repression of ribosome biogenesis under nutrient-limited conditions. *iScience* **25**, 103986 (2022).
41. Panasenko, O. O. & Collart, M. A. Presence of Not5 and ubiquitinated Rps7A in polysome fractions depends upon the Not4 E3 ligase. *Mol. Microbiol* **83**, 640–653 (2012).
42. Mori, K., Kawahara, T., Yoshida, H., Yanagi, H. & Yura, T. Signalling from endoplasmic reticulum to nucleus: transcription factor with a basic-leucine zipper motif is required for the unfolded protein-response pathway. *Genes Cells* **1**, 803–817 (1996).
43. Kawahara, T., Yanagi, H., Yura, T. & Mori, K. Endoplasmic reticulum stress-induced mRNA splicing permits synthesis of transcription factor Hac1p/Ern4p that activates the unfolded protein response. *Mol. Biol. Cell* **8**, 1845–1862 (1997).
44. Hu, Z., Killion, P. J. & Iyer, V. R. Genetic reconstruction of a functional transcriptional regulatory network. *Nat. Genet.* **39**, 683–687 (2007).
45. MacIsaac, K. D. et al. An improved map of conserved regulatory sites for Saccharomyces cerevisiae. *BMC Bioinforma.* **7**, 113 (2006).
46. Defenouillère, Q. et al. The induction of HAD-like phosphatases by multiple signaling pathways confers resistance to the metabolic inhibitor 2-deoxyglucose. *Sci Signal* **12** https://doi.org/10.1126/scisignal.aaw8000 (2019).
47. Anshu, A., Mannan, M. A., Chakraborty, A., Chakrabarti, S. & Dey, M. A novel role for protein kinase Kin2 in regulating HAC1 mRNA translocation, splicing, and translation. *Mol. Cell Biol.* **35**, 199–210 (2015).
48. Ghosh, C. et al. Phosphorylation of Pal2 by the protein kinases Kin1 and Kin2 modulates HAC1 mRNA splicing in the unfolded protein response in yeast. *Sci. Signal* **14** https://doi.org/10.1126/scisignal.aaz4401 (2021).
49. Karagöz, G. E., Acosta-Alvear, D. & Walter, P. The Unfolded Protein Response: Detecting and Responding to Fluctuations in the Protein-Folding Capacity of the Endoplasmic Reticulum. *Cold Spring Harb. Perspect Biol.* **11** https://doi.org/10.1101/cshperspect.a033886 (2019).
50. Benanti, J. A., Cheung, S. K., Brady, M. C. & Toczyski, D. P. A proteomic screen reveals SCFGrr1 targets that regulate the glycolytic-gluconeogenic switch. *Nat. Cell Biol.* **9**, 1184–1191 (2007).
51. Berset, C. et al. Transferable domain in the G(1) cyclin Cln2 sufficient to switch degradation of Sic1 from the E3 ubiquitin ligase SCF(Cdc4) to SCF(Grr1). *Mol. Cell Biol.* **22**, 4463–4476 (2002).
52. Mathur, R. & Kaiser, P. PCR-mediated epitope tagging of genes in yeast. *Methods Mol. Biol.* **1205**, 37–44 (2014).
53. Janke, C. et al. A versatile toolbox for PCR-based tagging of yeast genes: new fluorescent proteins, more markers and promoter substitution cassettes. *Yeast* **21**, 947–962 (2004).
54. Longtine, M. S. et al. Additional modules for versatile and economical PCR-based gene deletion and modification in Saccharomyces cerevisiae. *Yeast* **14**, 953–961 (1998).

55. Shedlovskiy, D., Shcherbik, N. & Pestov, D. G. One-step hot formamide extraction of RNA from Saccharomyces cerevisiae. *RNA Biol*. **14**, 1722–1726 (2017).
56. Inada, T. & Aiba, H. Translation of aberrant mRNAs lacking a termination codon or with a shortened 3′-UTR is repressed after initiation in yeast. *EMBO J*. **24**, 1584–1595 (2005).

Acknowledgements

The authors thank Dr. Tohru Yoshihisa, University of Hyogo, for providing antibody against the Hac1 protein and for critically reading the manuscript. The authors thank the members of their laboratories for discussions and critical comments on the manuscript. This work was supported by AMED (JP23gm1110010, JP223fa627001 to T.I.), MEXT/JSPS KAKENHI (Grant Numbers JP19H05281, 21H05277, 22H00401 to T.I., 21H00267, 23H04249 and 23K23869,18H05498 to Y.S.), Research grants from Takeda Science Foundation (T.I.), and JST PREST Grant Number JPMJPR21EE (Y.M.).

Author contributions

Genetic and biochemical experiments were performed by N.S., N.Y., Y.Mastuki, and S.T. under the supervision of T.I. N.S. performed the ribosome profiling experiments under the supervision of S.L, Y.Matsuo, and T.I. N.S. and T.I. wrote the manuscript. T.I. primarily conceived the idea and designed the experiments.

Competing interests

The authors declare no competing interests.

Additional information

Supplementary information The online version contains supplementary material available at https://doi.org/10.1038/s41467-025-57360-1.

Correspondence and requests for materials should be addressed to Toshifumi Inada.

Peer review information *Nature Communications* thanks Madhusudan Dey, Adrien Rousseau and the other, anonymous, reviewer(s) for their contribution to the peer review of this work. A peer review file is available.